



NANYANG
TECHNOLOGICAL
UNIVERSITY



Universität für Bodenkultur Wien

CO-TRANSLATIONAL INTEGRATION OF THE LIGHT HARVESTING COMPLEX II AND ITS ASSOCIATED PIGMENTS INTO POLYMERIC MEMBRANES

by
Zapf Thomas

University of Natural Resources and Life Science, Vienna,
Austria

Nanyang Technical University, Singapore, Singapore

Dissertation

Submitted in partial fulfilment of the requirements for the Doctor of Philosophy/PhD
degree

Supervisor: Prof. Dr. Eva-Kathrin Sinner

Co-Supervisor: Prof. Dr. Susana Geifman Shochat

Vienna, October 2015

Acknowledgments

I would like to express my sincere thanks to my supervisor Univ.Prof. Dr.rer.nat. Eva-Kathrin Sinner for accepting me as her doctoral student. I am grateful for all her support and guidance as well as giving me the freedom to follow my own ideas.

I also want to give my gratitude to my colleagues Darren Tan, Christian Zafiu, Christoph Zaba, Oliver Bixner, Tobias Reinelt and Christoph Huber for their support and helpful discussions.

Moreover I also want to thank my supervisor at the Nanyang Technical University, Assoc. Prof. Susana Geifman Shochat, for being such a wonder host, all her support, effort and our long discussions.

Further I want to thank my co-advisor Univ. Prof. Harald Paulsen, University of Mainz, Germany, for kindly providing the cDNA of LHCII, help with the chlorophyll preparation and his important feedback on my work.

I also want to thank the Ministry of Transportation and Innovation, BMVIT, Austria, for financial support of the International Graduate School, IGS.

Abstract

One of nature's most effective evolutionary concepts is to harvest and dissipate solar energy through the major light harvesting complex II (LHCII). This protein with its associated pigments is the main solar energy collector in higher plants. Our aim is to combine LHCII-pigment complexes with stable and highly controllable polymer-based membrane systems for future technological applications. We produced LHCII using wheat germ extract-based cell-free protein synthesis and show through Surface Plasmon Resonance (SPR,) Transmission Electron Microscopy (TEM) and Western blot the successful integration of LHCII and its pigments into polymersomic vesicles, called polymersomes. We further demonstrate by digestion assays an unidirectionality of LHCII insertion. Centrifugal microfiltration in means of polymersome purification as well as the development of a novel silica nanoparticles based purification method are further presented in this work. A silica nanoparticle based purification method was developed and optimized to meet our need of increased purification and harvesting efficiency of proteopolymersomes out of the crude cell-free lysate environment. Proper purification of synthesized proteopolymersomes was essential for further usage and subsequent characterization and analysis. Surface-modified silica nanoparticles with an antibody targeting the material of the polymer were able to bind and immunoprecipitate polymersomes and proteins by centrifugation. Analysis suggests that both purification methods did not compromise the polymersomic structure, nor their ability to retain integrated membrane protein. Comparison showed that immunoprecipitation was able to produce proteopolymersomes of greater purity and yield. Fluorescence measurements of purified proteopolymersomes indicate successful binding of pigments to the proteins within this new environment.

Surface Plasmon Resonance after cell-free synthesis on tethered polymer membranes indicates that LHCII is able to integrate functionally into planar bilayers. Surface Plasmon enhanced Fluorescence Spectroscopy reveals energy transfer from *Chl b* to *Chl a* which strongly suggests a native folding of the protein. Regeneration experiments showed that pigments harmed in their function through surface plasmon induced bleaching can be exchanged through incubation with fresh pigment solution.

Keywords: Light Harvesting Complex • Synthetic polymer membranes • Membrane protein expression

Zusammenfassung (Abstract in German)

Eines der wirkungsvollsten Konzepte der Natur ist die Aufnahme und Verwertung von Sonnenenergie durch den Lichtsammelkomplex II (LHCII). Dieses Protein, mitsamt den damit verbundenen Pigmenten, ist der Haupt-Sonnenenergiekollektor in höheren Pflanzen. Unser Ziel ist es, LHCII-Pigment-Komplexe mit stabilen und modifizierbaren Polymermembranen für zukünftige technologische Anwendungen zu kombinieren. Membranproteine wie der LHCII haben einen komplizierten Aufbau mit amphiphilen Eigenschaften. Ohne eine passende Einbettungsumgebung verlieren diese Proteine ihre Struktur und damit auch ihre Funktion. Wir produzierten LHCII mit Hilfe eines Weizenkeimextrakt basierten zellfreien Proteinsynthese Systems und zeigten durch Oberflächenresonanzspektroskopie (SPR), Transmissionselektronenmikroskopie (TEM) und Western Blot die erfolgreiche Integration von LHCII und dessen Pigmenten in Polymersomen. Außerdem konnten wir durch Verdauungsexperimente eine gerichtete Orientierung der LHCII Komplexe feststellen. Zur erfolgreichen Polymersomenaufreinigung wurde sowohl eine bereits etablierte Zentrifugations-Mikrofiltrationsmethode verwendet als auch ein weiteres alternatives und effizienteres Reinigungsverfahren, basierend auf Antikörper funktionalisierten Silikat Nanopartikel, entwickelt. Die Silikat Nanopartikel Methode wurde entwickelt, um den geforderten, hohen Ansprüchen, an Reinheit und Ausbeute, zu entsprechen, welche essentiell für nachfolgende Charakterisierungen und Analysen waren. Diese oberflächenmodifizierten Silikat Nanopartikel sind in der Lage, an den hydrophilen Teil des Polymer zu binden und ermöglichen somit eine auf Zentrifugation basierende Immunpräzipitation der Polymersomen. Untersuchungen zeigten, dass die beiden Reinigungsverfahren weder die Polymersomstruktur, noch ihre Fähigkeit integriertes Membranprotein zu behalten gefährden. Vergleichsanalysen ergaben, dass die Immunpräzipitation in einer größerer Reinheit und Ausbeute resultiert. Fluoreszenzmessungen von gereinigten Proteopolymersomen (Polymersomen mit integrierten Protein) zeigten erfolgreiche Bindung der Pigmente an die Proteine in diesem biomimetischen Umfeld.

Oberflächenplasmonenresonanzspektroskopie von oberflächengebundenen LHCII-Pigment Polymermembranen zeigte, dass LHCII in der Lage ist, funktionell in planare Doppelschichten zu integrieren. Oberflächen Plasmon verstärkte Fluoreszenzspektroskopie zeigte einen Energietransfer von *Chl b* zu *Chl a*, was stark darauf hindeutet, dass eine native Faltung des zellfrei generierten und

Polymermembrane integrierten LHCII Komplexes vorliegt. Regenerationsexperimente demonstrierten, dass Pigmente, die ansonsten durch Bleichungsprozesse in ihrer Funktion terminiert wurden, durch Inkubation mit einer frischen Pigmentlösung austauschbar sind.

Schlüsselwörter: Lichtsammelkomplex • Synthetische Polymermembranen • Membranproteinexpression

Table of Contents

1. Introduction	7
1.1. Light harvesting complex II	7
1.2. Polymer mimetic bilayers.....	14
1.3. Cell-free synthesis	16
1.4. The principle of Surface Plasmon Resonance (SPR) and Surface Plasmon-enhanced Fluorescence Spectroscopy (SPFS).....	18
2. Publications.....	21
2.1. Nanoscopic leg irons: harvesting of polymer stabilized membrane proteins with antibody functionalized silica nanoparticles	21
2.2. Functional Synthesis of the Light Harvesting Complex II into Polymeric Membrane Architectures	38
4. Conclusion	53
5. Abbreviations	56
6. List of Figures	58
7. References.....	60

1. Introduction

1.1. Light harvesting complex II

The process of light harvesting is present in all photosynthesizing organisms ranging from simple *Archea* to higher plants. Throughout evolution the core structure and function of the light harvesting complex has remained conserved.

The light-harvesting chlorophyll II (LHCII) is the main energy collector of photosystem II. The focus within this work will be on this particular complex, especially on the pea derived chlorophyll a/b binding protein AB80, further just described as LHCII, which is very well described in literature. It has 269 amino acid residues including a 37 amino acid signal domain at the N-terminus which guides the protein from the cytoplasm into the chloroplast.¹ The main role of the whole series of LHCII-pigment proteins is to harvest photonic energy by absorbing photons of certain energy levels. Within all green plants, LHCII is found in the thylakoid membrane of the chloroplasts, and it is most likely the most abundant membrane protein in the world. Different types of LHCII are classified depending on their pigment composition and their exact size.² In nature LHCII is commonly found in a trimetric state. However, when reconstituted or treated with phospholipase in presence of high detergent concentration, it can become monomeric.³ A monomeric LHCII protein strongly binds 13-15 chlorophyll (*Chl a* and *Chl b*) molecules⁴ and 3-4 carotenoids.⁵

In vivo, the LHCII assembly is triggered by the initial binding of pigments to the protein to form monomers first, before forming trimetric or higher-order oligomeric states when under continuous light exposure.⁶

LHCII can be isolated from plant material. One method is by solubilizing the thylakoid membrane with Triton X-100 and octyl glucoside followed by an octyl glucoside-sucrose gradient centrifugation.⁷ Sprague *et al.* successfully demonstrated the reconstitution of plant derived LHCII into both phosphatidylcholine liposomes as well as into digalactosyldiglyceride liposomes.⁷ Furthermore, Paulsen *et al.* cloned the LHCII coding gene AB80 into a bacterial vector and expressed it within an *E.coli*. Subsequent reconstitution of the protein with its pigments resulted into a similar spectroscopic behavior as isolated LHCII.⁸ Complete refolding of the denatured protein under renaturing conditions occurs only in the presence of the pigments. This demonstrates the importance of the pigments within the folding process.⁹

Booth and Paulsen determined the kinetics of the *in vitro* assembly through time resolved fluorescence spectroscopy monitoring the LHCII bound chlorophyll fluorescence. Two main assembly steps were found, a faster one between 30 - 60 seconds and a slower one of several minutes. In the first step, a loose intermediate protein-pigment construct is formed while the formation of functional LHCII is completed by establishing energy transfer between *Chl b* and *Chl a* in the second step.¹⁰ The kinetic formation steps are dependent on the concentration and composition of the pigments. *In vitro* an occupation of the majority of chlorophyll binding pockets with *Chl a* accelerates the process, showing a more dominant binding. However, this also results in reduced stability. Later it was also found that the xanthophyll concentration has a significant impact on the formation kinetics with lutein being the strongest accelerator.¹¹

LHCII is one of the few membrane proteins for which a high resolution ultrastructure has been elucidated.¹²⁻¹³ LHCII consists of three transmembrane α -helices which serve as a scaffold for the tight packaging of the pigments. Without this unique scaffold architecture the pigments would aggregate and harvesting of solar energy would not be possible.¹² The local chlorophyll concentration within the thylakoid membrane is extremely high, reaching up to 300 mM.¹² The pigments bind to certain binding sites of the LHCII protein which are defined by the amino acid sequence and folding structure.¹⁴ Within the chloroplast, LHCII is integrated into the membrane always in the same direction, the N-terminus is in the stroma while the C-terminus protrudes into the lumen.¹²

The full length protein with its transit peptide sequence has a mass of 28 654 Da.¹⁵ Kühlbrandt *et al.* using electron crystallography had revealed already in 1994 that LHCII consists of three transmembrane α -helices, a short amphiphilic helix, at least 12 chlorophylls and two carotenoids.¹⁶ More recent findings achieved by x-ray crystallography gave a more detailed picture of the pigment-LHCII complex. It revealed the exact position and specific binding sites of all 14 chlorophylls found in monomeric LHCII. The chlorophylls were characterized as eight *Chl a* and six *Chl b* (Figure 1). While the carotenoids were identified as two luteins¹³ and one neoxanthin while the fourth member was shown to be violaxanthin.¹² Two of the transmembrane α -helices proved to be unusually long (helix 1 and 4), they are linked through a shorter slightly curved transmembrane helix (helix 3). On the luminal side, two small

amphiphilic helices (helix 2 and 5) were found which link helix 1 and 3 together as well as helix 4 with the C-terminus. The two long helices 1 and 4 are interlocked by salt bridges, making this part of the complex rigid.¹²

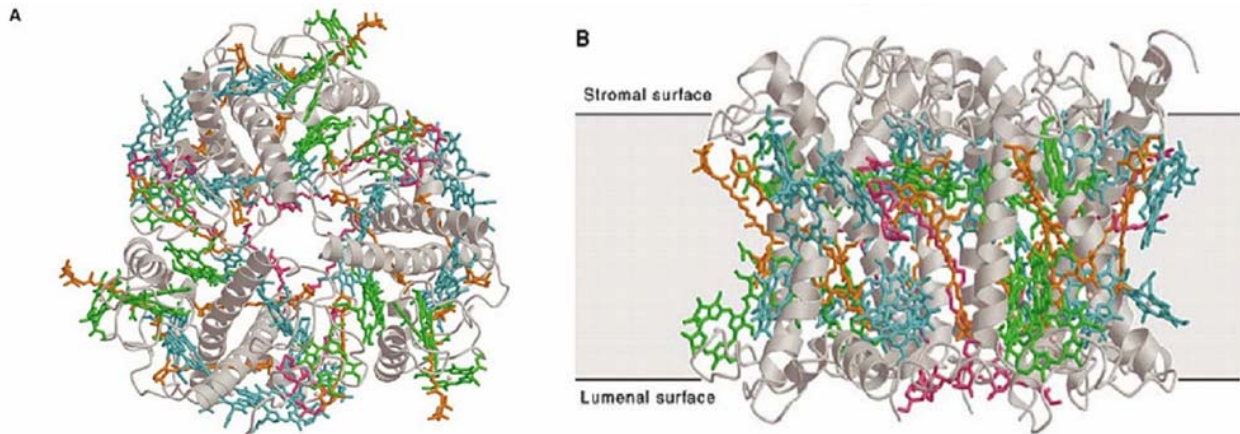


Figure 1: Model of the quaternary structure of LHCII trimers. A) View from stromal side on a LHCII trimer with all the chlorophylls and carotenoids tightly packed. In B) the integration into the thylakoid membrane is shown.¹² (adapted from “Crystallisation, structure and function of plant light-harvesting Complex II.”, by Barros, T. & Kühlbrandt, W., 2009, Biochim. Biophys. Acta BBA - Bioenerg. 1787, 753–772)

Furthermore the α -helices formation in LHCII under reconstitution conditions of denatured protein *in vitro* is linked to the binding of the pigments. It was shown that the α -helix content increases in two kinetic steps when reconstituted. Depending on carotenoids concentration, the helix formation time is reduced in the presence of only low amounts of carotenoids.¹⁷ No preformed α -helix or any other secondary structure is necessary for the successful renaturation *in vitro*.¹⁸ A refolding *in vitro* is possible with *Chl a* as the only chlorophyll. However some of the chlorophyll binding sites must be occupied by *Chl b* to achieve complex stability. Interestingly the LHCII stability is also strongly related to the binding of certain carotenoids, for example, lutein has the best stabilizing effect while LHCII with neoxanthin as the only carotenoid is very unstable.¹¹ In nature, the xanthophyll zeaxanthin is only found in LHCII under light-stress conditions.¹⁹

The size of a monomer resolved by electron crystallography was 30 Å by 50 Å with a thickness of 60 Å.²⁰ The trimeric dimensions, revealed by X-ray crystallography with

a resolution of 2.72 Å, show a spherical shell with an outer diameter of 261 Å and an inner one of 160 Å.¹³

The pigments associated with the LHCII scaffold are different in their structure, behavior and binding strength. As described earlier, the two chlorophylls found within the LHCII are *Chl a* and *Chl b*, as shown in Figure 2. The structure of these molecules is almost similar except for one side chain. The difference in this side chain results in altered fluorescence and binding properties.

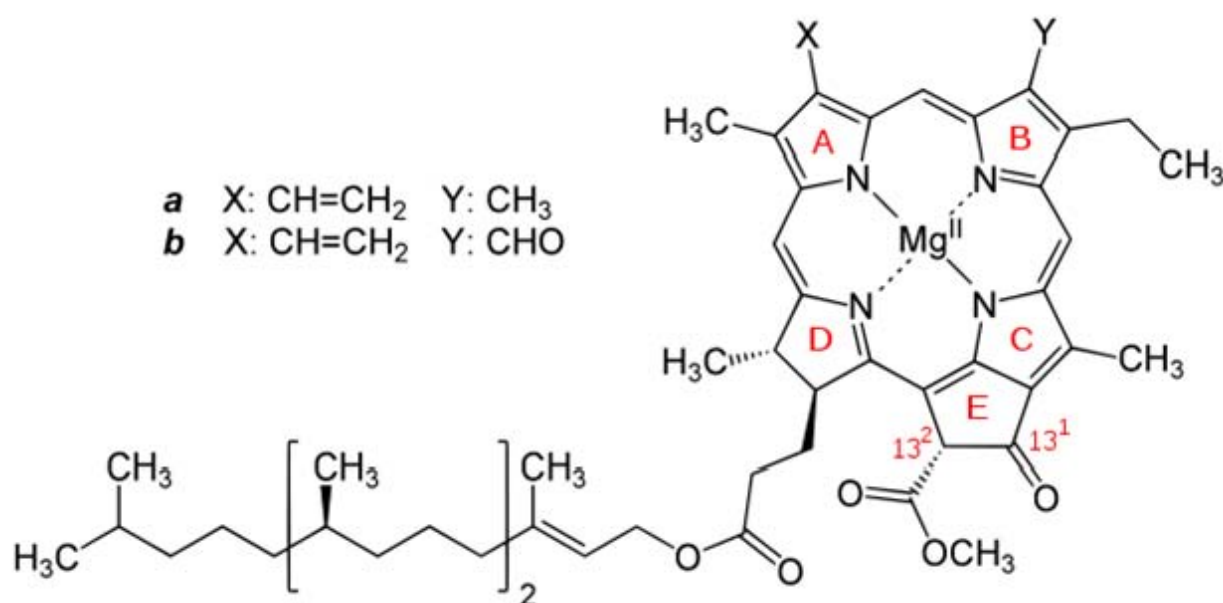


Figure 2: Core structure of chlorophyll *a* and *b*. Only one side chain is different between *Chl a* and *Chl b* which results into altered binding properties as well as a shift in the adsorption and emission spectra.²¹ (adapted from “Chlorophyll a, b and d.” by Yikrazuul, 2009, http://commons.wikimedia.org/wiki/File:Chlorophyll_a_b_d.svg)

The *chlorophylls* bind *via* the magnesium ion, in their center, to a ligand with a free electron pair, such as nitrogen or carbonyl oxygen which is normally provided by an amino acid of the protein. It can also bind to a water molecule H-bonded to a main chain carbonyl of the LHCII protein. In the case of *Chl₇*, the binding is coordinated by a phosphatidylglycerol while for *Chl₁₀*, the needed oxygen electron pair is provided by an already bound *Chl₁₃* molecule. Most of the binding sites within the protein are conserved throughout the different types of LHC. The specificity of the *Chl a* or *Chl b* binding site is defined by the presence of a hydrogen bonding partner for the *Chl b*

formyl group.¹² It is possible under *in vitro* condition to force *Chl a* into a *Chl b* binding site and vice versa.²² However, under natural circumstances no sign of a mixed binding to the specific binding sites is observed.

Chl a appears to be the oldest chlorophyll from an evolutionary point of view for it is needed for the production of *Chl b*. *Chl b* is synthesized from *Chl a* via chlorophyllide an oxygenase and chlorophyll synthase. In case of *Chl b* catabolism, it is first reconverted into *Chl a* before further catabolization.²³

The absorbance spectrum of LHCII is mainly shaped by the chlorophylls which display two absorption maxima, a stronger and a weaker one. As shown in Figure 3, *Chl a* has its maxima at around 430 nm and 661nm while *Chl b* exhibits its maxima at around 450nm and 645 nm. Chlorophyll not only absorbs photons but in cases where energy transfer to the reaction center of the photosystems is inhibited, it can emit light at certain wavelengths, *Chl a* at 680nm and *Chl b* at 660nm. The spectra depends on the surrounding fluid and can shift in different solutions.²⁴

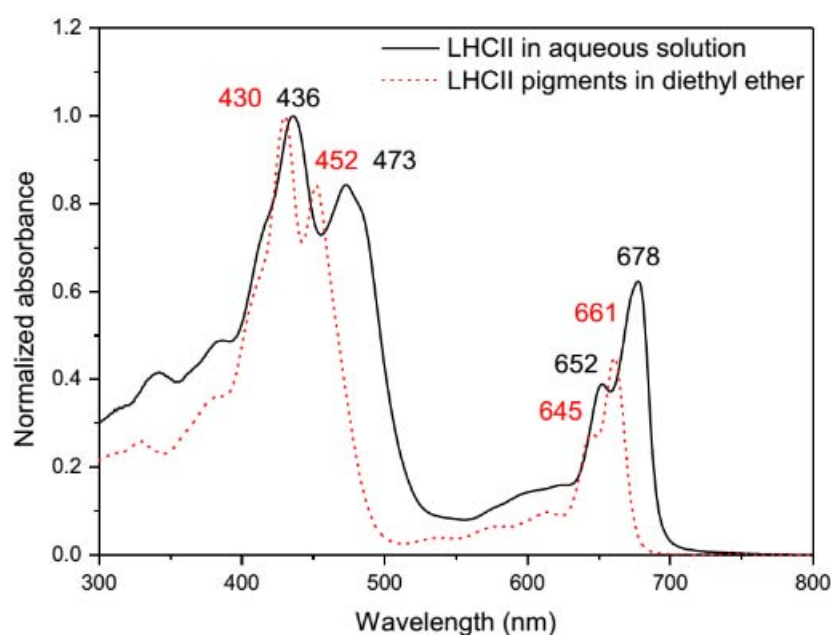


Figure 3: LHCII-pigment absorbance spectra within an aqueous solution as well as in diethyl ether. The main absorbance occurs within the blue and red light range.²⁴ (adapted from “Photocurrent activity of light-harvesting complex II isolated from spinach and its pigments in dye-sensitized TiO₂ solar cell”, by Yu, D., Zhu, G., Liu, S., Ge, B. & Huang, F., 2013, Int. J. Hydrog. Energy 38, 16740–16748)

As described earlier not only chlorophylls bind to LHCII but also different types of carotenoids which contribute to the light harvesting, facilitating stabilizing effects and probably most importantly, protecting against photo oxidative damage. Under normal circumstances the LHCII contains lutein, neoxanthin and violaxanthin. The LHCII crystal structure shows two lutein molecules intertwined between the two long transmembrane α -helices, strongly indicating a stabilizing effect of lutein for the LHCII.¹⁶ Lutein binds strongly to two inner binding sites of the LHCII whereas violaxanthin has only a weak binding to a peripheral binding site. Violaxanthin can easily dissociate from isolated LHCII, indicating low importance for stabilization.⁵ In lutein/neoxanthin, lutein/violaxanthin and lutein/zeaxanthin competition experiments, it was shown that two binding sites are rather selective for lutein with the lowest selectivity for zeaxanthin.¹⁹

LHCII bound carotenoids have several functions, one of them is to increase absorbance efficiency by broadening the absorption spectra and transferring the excitation energy to a chlorophyll molecule from where the energy can be forwarded via another *Chl a* to the reaction center of photosystem II. Close contact between the pigments is needed to achieve energy transfer from the carotenoids to the chlorophylls as well as from one chlorophyll to the next without significant loss of energy.²⁵ This energy transfer as shown in Figure 4 from carotenoid to chlorophyll is rapid (<100 fs) and occurs mainly to *Chl b* in a first step and is then transferred to *Chl a* in a second step.²⁶

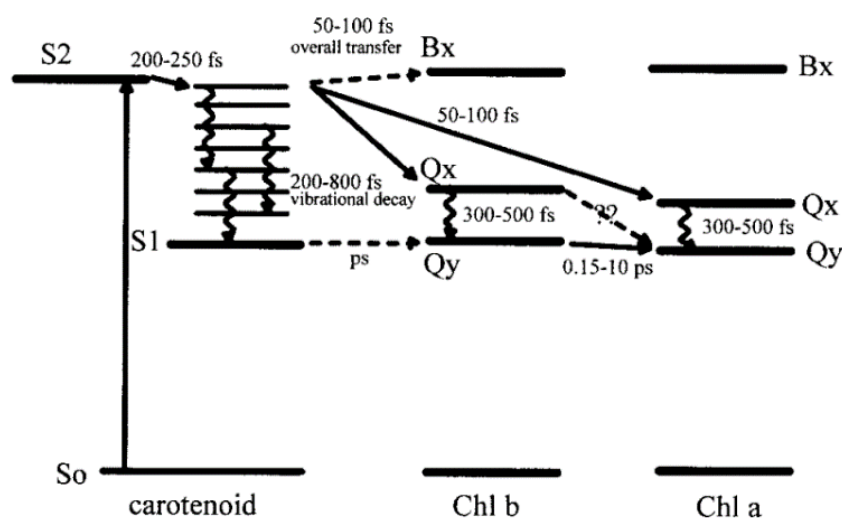


Figure 4: Energy transfer from carotenoids to chlorophylls and their different excitation levels and transfer times.²⁶ (adapted from "Carotenoid-to-chlorophyll energy transfer in recombinant major light-

harvesting complex (LHCII) of higher plants. I. Femtosecond transient absorption measurements", by Croce, R., Muller, M. G., Bassi, R. & Holzwarth, A. R., 2001, *Biophys. J.* 80, 901–915)

When purified LHCII is reconstituted with pigments, in the absence of other proteins of the photosystem, the photonic energy can still be harvested and transferred from carotenoids to *Chl a/b* and from *Chl b* to *Chl a* but not further to a reaction center. Therefore the energy is emitted from *Chl a* as a photon with a higher wavelength in order to return to an unexcited state. This phenomenon can be used to test the functionality of reconstituted LHCII, as *Chl b* that becomes excited at a wavelength of 460 nm or 640 nm and would emit light at a wavelength of 660 nm. However, within a tightly pigment packed LHCII the energy will be transferred to *Chl a* and emitted at a higher wavelength of around 680nm. In vivo, *Chl b* is non-fluorescent due to 100% efficient energy transfer to *Chl a*.²⁷ This energy transfer only occurs in correctly folded pigments functionalized LHCII.⁸

1.2. Polymer mimetic bilayers

Membrane proteins such as LHCII are not only interesting for their study only, but bear the possibility of technological usage. However, the fragility of the lipid membrane is a major drawback. Membrane proteins have sophisticated structures displaying amphiphilic characteristics. Without a suitable support the structure and hence their functions are lost. Attempts have been made to replace lipid membranes with amphiphilic polymeric membrane mimics allowing for a more stable embedding environment as compared to conventional lipid membranes.²⁸ Incorporation of various membrane proteins into such artificial supports has been successfully demonstrated several times, including GPCRs²⁹ and other membrane proteins^{30,31}.

Those polymeric membranes mimic the amphiphilic nature of lipid membranes and can be formed through the usage of amphiphilic diblock^{28,32,33} or triblock copolymers³⁴. At appropriate concentrations in aqueous solutions, they self-assemble into bilayered membrane vesicles called polymersomes.^{28,32,33} Noteworthy, different self-assembled constructs can be favored depending on the architecture of the block copolymer. These include spherical micelles, cylindrical micelles or polymersomes as shown in Figure 5.³⁵ Furthermore, thermo-reversible transition from tubular polymersomes to vesicular structures has also been observed.³⁶ Even more sophisticated structures such as helical cylindrical micelles³⁷ have been reported. This increases the spectra of possibilities but it also makes a careful selection of the appropriate polymers for each purpose essential.

Polymer membranes are also easily tunable in their permeability, rigidity, thickness and stability via selection of different polymeric building blocks.^{33,38–40} Functionalization and targeted modification of the polymer further increases its application spectra.^{41,42} Cross-linked polymersomes have shown to be stable enough to withstand solvents such as chloroform⁴³, opening novel possibilities unachievable by lipid membranes. The usage of poly(ethylene) glycol (PEG, also called PEO – polyethylene oxide) as a hydrophilic domain, in cases of *in vivo* applications, ensured prolonged *in vivo* circulation times and enhanced stability.³⁸ PEGylated constructs gain a certain “stealth” character due to steric repulsion and reduced interfacial free energy.⁴⁴

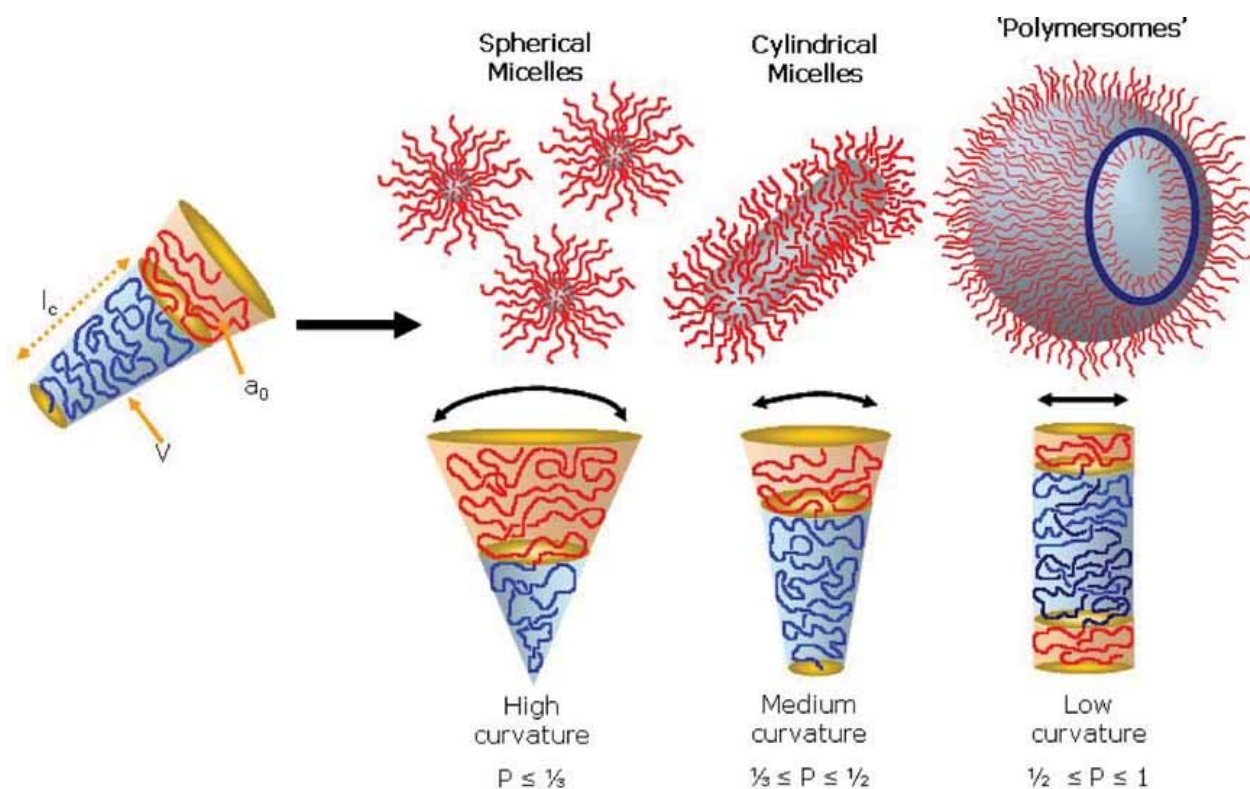


Figure 5: Main self-assembled structures formed by AB diblock copolymer. Depending on the dimensionless 'packing parameter' p either spherical micelles, cylindrical micelles or polymersomes form in the appropriate concentration and solution.³⁵ (adapted from „Self-Assembled Block Copolymer Aggregates: From Micelles to Vesicles and their Biological Applications”, by Blanazs, A., Armes, S. P. & Ryan, A. J., 2009, *Macromol. Rapid Commun.* 30, 267–277)

For the formation of polymersomes, similar techniques as used for liposomes formation, such as film or bulk rehydration^{45,46}, electroformation²⁸ or water addition/solvent evaporation method⁴⁷, can be used. Polymersome size can be reduced and adjusted through sonication, extrusion or freeze-thaw cycles. Creation of unilaminar polymersomes are also created using these methods.^{45,46}

Similar to lipid membranes, polymer can also form planar bilayers making it even more attractive for technological applications.^{42,48}

Within this presented work the focus will be on the usage of polybutadiene₁₂₀₀(PBD)-poly(ethylene)glycol₆₀₀(PEO) co-block polymer which has been shown to be capable of supporting membrane proteins.^{29,31}

1.3. Cell-free synthesis

So far, membrane protein synthesis involved massive bending of the cellular biochemistry in order to produce membrane proteins in significant amounts. Expression of membrane proteins in a living host represents a difficult task due to the highly complex structure, hydrophobic domains and cytotoxic effects upon integration into the membrane which causes the achievable yield to be reduced dramatically. Another limiting factor is the possible aggregation of proteins within the host which often leads to misfolding and protein aggregation, altering the protein's functionality. Furthermore, detergents and substantial efforts for purification are often needed besides a generally low refolding efficiency and insertion into a biomimetic membrane structure.

A method to circumvent the issues arising from membrane protein synthesis within living host cells is the usage of so called cell-free synthesis consisting of crude cell lysate based extract. The usage of cell extracts for the expression of proteins is well known for decades, such as *E.coli* derived systems.⁴⁹ The lysate represents an 'open' system that allows - to a certain extent - the control of the synthesis conditions and bypassing cellular regulation mechanisms. For cell-free expression of membrane proteins, the key idea is the addition of lipids, detergents and other membrane mimic supports to solubilize the protein upon its production.⁵⁰ The successful introduction of a suitable embedding environment, e.g. liposomes,^{51,52} polymers³¹ or detergents,⁵³ for stabilizing the amphiphilic membrane proteins have been demonstrated.

The cell-free expression of membrane proteins into liposomes, polymersomes, tethered membranes and nanodiscs is growing into an emerging field.^{54,31} It bears the potential of generating quantitative, robust and sustainable membrane protein investigation platforms for fundamental research as well as for applied sensor developments and actuation tasks such as protein based solar cells. Several different cell-free protein expression systems have been developed ranging from prokaryotic organisms as *E. coli*⁵⁵ to eukaryotic organisms such as yeast⁵⁶, wheat germ⁵⁷, insect cells^{58,59} and mammalian cells^{60,61}. In order to circumvent the issue of using ill-defined crude cell extracts very well defined and characterized systems based on recombinantly expressed proteins are emerging.⁶² Due to the abundance of different cell-free systems, it is possible to choose the most suitable system for each protein in respect to complexity and post translational modifications. A few examples for

successful expression of membrane proteins into membrane supports using cell-free systems, are the human dopamine D2 receptor⁶³, human claudin-2³¹, GPCRs²⁹ as well as many more^{51,64}.

The expression within these systems is based either directly on added mRNA or on DNA which is transcribed *in vitro* simultaneously and then followed by translation. Due to the high efficiency and high yield that can be achieved through cell-free synthesis, even PCR products can be used for successful protein production without the need for time consuming transformation into a host organism. Another important advantage in the usage of cell-free synthesis is the strongly reduced time factor needed for the protein expression.⁵⁰ Most commonly used cell-free systems are single patch reactions where the reaction time is limited by the depletion of resources and accumulation of inhibitory byproducts.⁶⁵ Continuous⁶⁶ and semicontinuous⁶⁷ systems have been developed to address this issue. However, its impact on the scientific community has been low so far. Presented in this work is the commercially available wheat germ based system, L4140 from Promega.

1.4. The principle of Surface Plasmon Resonance (SPR) and Surface Plasmon-enhanced Fluorescence Spectroscopy (SPFS)

Surface Plasmon Resonance is a phenomenon created by polarized light hitting a metal film at the interface of materials with different refractive indices, usually a metal and a dielectric surface. Surface plasmons are resonant electromagnetic oscillations of conduction electrons at the interface of the metal and dielectric surface. The resonance behavior is induced by incident photons, emitted by a light source (e.g. laser).⁶⁸

Excitation needs a coupling medium, normally a glass prism, as the momentum of the surface plasmons at the metal-dielectric interface is greater than the momentum of light. If light passes through a block of glass, its momentum is increased allowing a matching resonance of the plasmons, depending on the angle of incidence.⁶⁸

Two different approaches for exciting surface plasmon waves exist, the Otto setup and the Kretschmann configuration. Within Kretschmann configuration, a glass block is coated on one side with a thin layer of metal. Light entering the glass block creates plasmon excitation on the other side of the metal film which itself creates an evanescent field that passes through the metal film.⁶⁸ A commonly used Kretschmann setup is schematically shown in Figure 6.

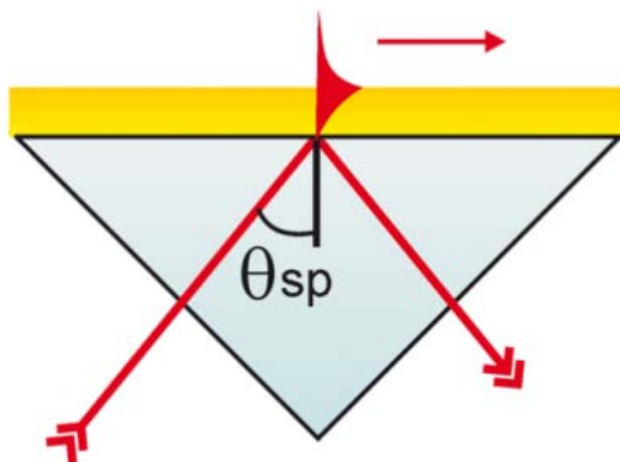


Figure 6: Schematic illustration of a Kretschmann configuration showing the propagation of surface plasmons and the resulting evanescence field on the outer side of the gold layer. The incident angle θ has to be chosen so that there is a phase match of the momentum of the light and the surface plasmons.⁶⁹ (adapted from “Localized surface plasmon resonances in nanostructures to enhance nonlinear vibrational spectroscopies: towards an astonishing molecular sensitivity”, by Lis, D. & Cecchet, F. , 2014, *Beilstein J. Nanotechnol.* 5, 2275–2292)

Commonly a thin 50 nm gold layer is used, but other metals such as silver can be used too. Depending on the chosen material the excitation wavelength of the light source needs to be adjusted to induce plasmon formation within the metal. Depending on the angle of incidence of the light, different levels of excitation can be achieved whereas at a certain angle, the so called SPR-angle, most photonic energy is absorbed by the resonating electrons on the interface. This angle is measured, when the intensity of reflected light reaches a minimum. If the surface properties of the interface change, the SPR-angle will change likewise. In SPR sensor technology this phenomenon is used to monitor binding interactions. The angular shift can be used to calculate the optical thickness of the binding layer. If the change in reflective intensity is measured as a function of the scattering angle, real time monitoring of surface changes can be done for both chemical and biological sensor applications.⁷⁰ For real time monitoring, the reflective intensity is measured at a certain angle within the linear part of the SPR curve as shown in Figure 7 due to the strong changes in reflective intensity upon surface changes. The total internal reflection resembles the point at which 100% of the light is reflected.

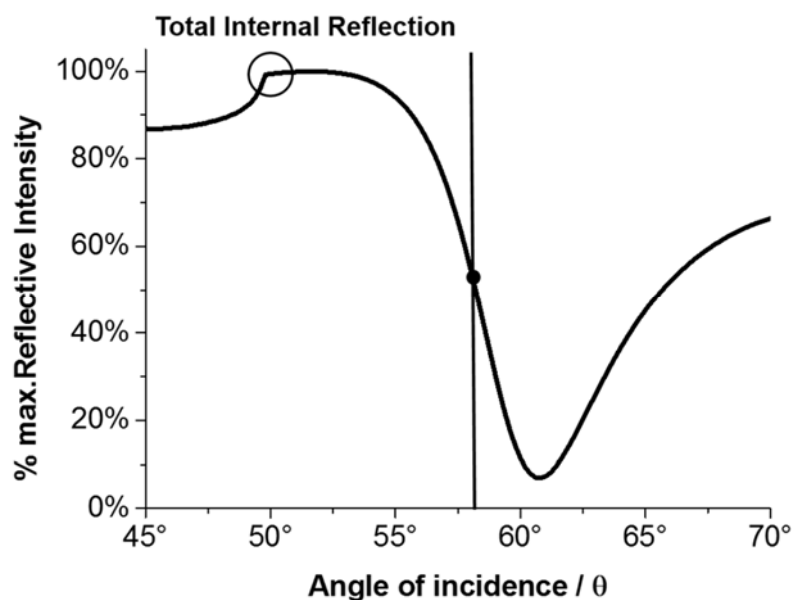


Figure 7: Representative SPR curve. The total internal reflection resembles the point at which 100% of the light is reflected. The black line crossing the curve in the point of the black circle demonstrated a suitable angle for real time measurements due to strong changes in signal intensity upon surface changes. At the point of the lowest reflective intensity the surface plasmon resonance is the strongest.

A big advantage of real time SPR monitoring is that it is a label free technique for the analysis of binding events such as antibody-antigen interactions – one of them is to be pre-deposited on the surface. SPR has proven to be an extremely sensitive method, allowing also the detection of low molecular weight molecules^{71,72}.

To further increase the sensitivity of SPR technology a combination with fluorescence spectroscopy can be done, taking advantage of the fact that fluorophores can be excited by the evanescent field created by the surface plasmons, achieving far greater sensitivity⁷³ than SPR on its own. To achieve excitations of the fluorophores they need to be within the decay length of the evanescent field which can be up to 200 nm^{74,75}.

2. Publications

2.1. Nanoscopic leg irons: harvesting of polymer stabilized membrane proteins with antibody functionalized silica nanoparticles

Authors:

Thomas Zapf, Christian Zafiu, Christoph Zaba, Cherng-Wen Darren Tan, Walter Hunziker
and Eva-Kathrin Sinner

Journal:

Biomaterial Science, Issue 9, 2015

Received: 23 Apr 2015

Accepted: 08 Jul 2015

First published online: 27 Jul 2015

DOI: 10.1039/C5BM00133A

Motivation:

The motivation and aim of this work is to exploit the structure and function of polymer-embedded membrane protein complexes for possible technological usage. Membrane proteins are notoriously difficult protein species to investigate and work with, due to their amphiphilic structure. A major drawback of membrane proteins is their dependence on bilayered membranes for correct folding and functioning.

Through the usage of *in vitro* membrane-assisted protein synthesis (iMAPS), we achieve a directed co-translational insertion³¹ of membrane proteins into polymersomes which mimic the cellular membrane. This circumvents the issues arising from a random insertion orientation through reconstitution. However, iMAPS – involves cell lysates, which inherently comprise a complex environment containing membrane remnants, soluble proteins and metabolites of various kinds. As such, it becomes necessary to apply drastic purification procedures.

So far, liposomes and proteoliposomes are often purified using methods suffering from either the need for dilution of the desired protein or the need for unnatural modification of the original protein structure through the addition of affinity tags. The non-invasive method of centrifugal microfiltration has already been used to purify membrane proteins integrated into polymersomes.³¹ However, sample loss and remaining contaminating cell-free lysate material interfering with the structural – functional integrity of the membrane protein of interest let us to the development of a novel polymersome purification strategy.

We demonstrate the successful usage of an immunoprecipitation strategy based on silica nanoparticles surface-modified with antibodies that have been raised against the hydrophilic part of the polymer material or the membrane protein itself. These modified Nanoparticles were effectively able to harvest polymersomes, proteopolymersomes and protein from the surrounding cell-lysate.⁷⁶

Nanoscope Leg Irons: Harvesting of Polymer-stabilized Membrane Proteins with Antibody – Functionalized Silica - Nanoparticles

Received 23 Apr 2015,

Accepted 08 Jul 2015

First published online 27 Jul 2015

Thomas Zapf^a, Christian Zafiu^b, Christoph Zaba^a, Chong-Wen Darren Tan^a, Walter Hunziker^c and Eva-Kathrin Sinner^a

DOI: 10.1039/C5BM00133A

www.rsc.org/

Silica – based nanoparticles (SiNPs) are presented to harvest complex membrane proteins, which have been embedded into unilamellar polymersomes *via* membrane assisted protein synthesis (iMAPS). Size – optimized SiNPs have been surface-modified with polymer – targeting antibodies, which are employed to harvest the protein – containing polymersomes. The polymersomes mimic the cellular membrane. They are chemically defined and preserve their structural – functional integrity as virtually any membrane protein species can be synthesized into such architecture *via* the ribosomal context of a cellular lysate. The SiNPs resemble ‘heavy leg irons’ catching the polymersomes in order to enable gravity – based, generic purification and concentration of such proteopolymersomes from the crude mixture of cellular lysates.

The cell-based production of membrane proteins comes always along with issues of, aggregation, misfolding, often low yield expression and potential cytotoxicity. Mastering those issues, purification often requires lysis of cells and keeping the membrane proteins in solution by the use of surfactants^{1,2}. However, the membrane proteins most often lose structural – functional integrity and are often degraded by proteases. Characterization and long term storage plans are often rendered impossible when it comes to the class of membrane proteins. At present, careful selection of the reconstitution methods used for protein production.³ As an alternative to surfactant stabilization, we present cell-free synthesis and co-translational insertion of membrane proteins into artificial membranes as an interesting alternative^{4–6}. We introduced the method as *in vitro* membrane-assisted protein synthesis (iMAPS) replacing lipid membranes by polymer membranes^{7–10}. Such polymeric membranes self-assemble into the form of robust 2D structures^{8,11} that can either be tethered to a surface, or formed into spherical vesicles often referred to as polymersomes^{8,9,12}. These have successfully even been applied as antigen presenting matrix for vaccination by Nallani et al.¹³ in combination with conventionally reconstituted membrane protein species.

However, iMAPS – involves cell lysates, which inherently comprise a complex environment containing membrane remnants, soluble proteins and metabolites of various kinds. As such, it becomes necessary to apply drastic purification measures. So far, liposomes and proteoliposomes, which are lipid vesicles with membrane proteins embedded, had been available – those are often purified using density gradient ultracentrifugation^{14–16} or high-speed ultracentrifugation¹⁷. These methods suffer from either dilution of the desired protein or in disintegration as liposomes are exposed to destructive shear forces over extended periods of time^{14–17}. Alternatively, without shear forces being involved, one could purify His₆-tagged membrane proteins using Ni-NTA supports^{10,18} or membrane protein-GFP fusion constructs for fluorescence detection size-exclusion chromatography¹⁹. Choosing polymeric membrane analogues, we presented the application of centrifugal microfiltration (involving the commercially available Amicon® filters) in order to purify proteopolymersomes from cellular lysates. The method of centrifugal microfiltration and as such has recently been reported by us to be useful in the purification of membrane proteins integrated into polymersomes⁶. However, recent problems with remaining contaminating materials corrupting the structural – functional integrity from the membrane protein of interest pushed us in the development of a novel strategy for proteopolymersome purification.

We propose using a modified immunoprecipitation strategy based on silica nanoparticles decorated with antibodies that have been raised against the respective polymer material forming the proteopolymersomes. In our case, anti-PEG antibodies, targeting the polymer itself, and anti-VSV antibodies, able to bind to the used proteins, were immobilized onto the surface of colloidal silica nanoparticles (SiNPs). The resulting antibody-functionalized SiNPs are effectively used for ‘harvesting’ the membrane protein species of interest. Following the one-step membrane protein synthesis procedure facilitated by iMAPS, such modified SiNPs are added to the iMAPS reaction mix and allowed to bind their targets (Fig. 1).

^a Department for Nanobiotechnology
Institute of Synthetic Bioarchitectures
University of Natural Resources and Life Science
Muthgasse 11/2, 1190 Vienna, Austria.
E-mail: eva.sinner@boku.ac.at

^b ICS-6 Structure Biochemistry
Forschungszentrum Jülich
Wilhelm-Johnen-Straße, 52425 Jülich, Germany.

^c Institute of Molecular and Cell Biology
A*Star, Singapore
61 Biopolis Drive, Proteos, 138673 Singapore.

Electronic Supplementary Information (ESI) available. See
DOI: 10.1039/C5BM00133A

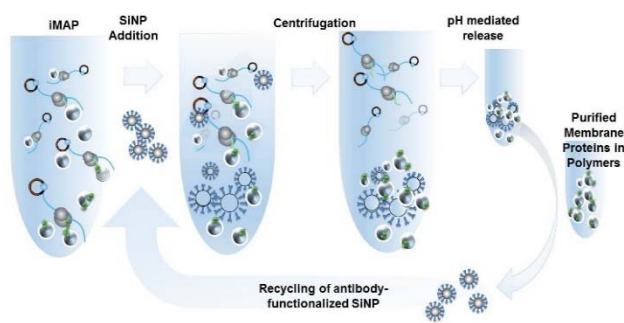


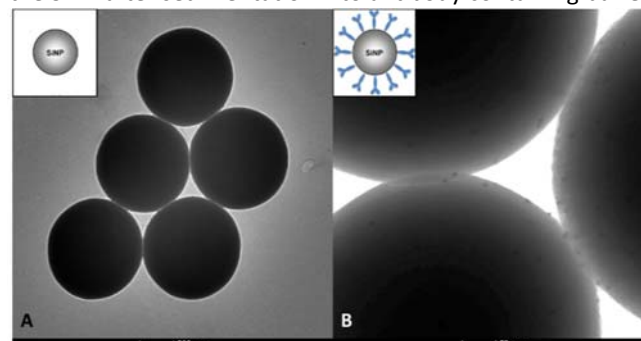
Fig. 1 Schematic overview of iMAP in presence of polymersomes, followed by addition of anti-polymer – functionalized silica nanoparticles (SiNP). Centrifugation of the SiNP with attached proteopolymersomes results in sedimentation of SiNPs with attached proteopolymersomes. Removal of supernatant containing cell lysate components followed by a pH - mediated dissolving of immunocomplex, harvesting of purified proteopolymersomes and regeneration of antibody - functionalized SiNPs for repeating cycles.

Subsequently, the SiNPs would facilitate sedimentation of the immunocomplexes, made from SiNPs and proteopolymersomes, using centrifugation at forces below 1, 700 x g over periods of only minutes. Acidic (10 mM Glycine/HCl, pH 2) as well as alkaline (10 – 100 mM NaOH, pH 12-13) treatment is subsequently carried out in order to dissolve the immunocomplex and ‘free’ the proteopolymersomes from the nanoparticle load (see supporting information). The resultant proteopolymersomes are subjected to further characterization procedures. Those harsh release conditions were chosen to ensure an efficient release as well as to reduce the non-specific protein adsorption to the polymer surface.

SiNP were synthesized using Stöber’s method²⁰ resulting in spherical, monodisperse particles (see Fig. 2). SiNP with a diameter of about 550 nm were synthesized by an appropriate selection of NH_3 , H_2O and tetraethyl orthosilicate in ethanol. This size was ideal for our use as the nanoparticles were small enough to maintain colloidal stability in PBS, yet provided sufficient mass to enable centrifugation at low forces achievable with standard table-top centrifuges. Furthermore, being three fold larger than the 200 nm polymersomes, the interstices of densely-packed SiNP would still provide sufficient space for polymersome integrity and interaction. In the preparation procedure of the polymersomic giant unilamellar vesicles (pGUVs) we added sucrose as this has been described to enhance stability²¹. Furthermore due to formation of huge immunocomplexes, observable by phase contrast microscopy, a lower centrifugal speed was applicable for pGUVs than for 200 nm sized polymersomes.

The SiNP produced were modified with 3-aminopropyl (trimethoxy) silane (APTES) to introduce primary amine groups, suitable for peptide coupling chemistry for antibody binding (Fig. 2A). In the next step, an incubation of the SiNP with 1-ethyl-3-(3-dimethylaminopropyl) carbodiimide (EDC) and N-hydroxysuccinimide (NHS) was performed. These compounds usually activate carboxylic groups, such as are found in proteins, in order to form peptide bonds with amine groups. However in order to prevent crosslinking between antibodies molecules, we decided to treat only the

silica nanoparticle surface instead. We immersed the SiNP in EDC/NHS 0,5M and 0,1M in H_2O for 10 min, and transferred the SiNP after sedimentation into antibody containing buffer



solution. This procedure resulted in presence of EDC and NHS only in the unstirred layer being around the surface of the SiNP resulting in covalent binding only when antibodies were in close proximity to the SiNP surface and not among each other. Deactivation of residual active groups was achieved by incubation with 1 M ethanolamine for another 10 min. Surface modifications to the nanoparticles were monitored by zeta potential analysis and were represented as changes in the surface charge (see ESI). Dynamic light scattering yielded a hydrodynamic diameter for the unmodified SiNP of about 540 nm.

Fig. 2 A: TEM of SiNP surface-modified with APTES and mouse α -VSV antibodies (Sigma). B) TEM of SiNP after binding of immunogold-labelled goat anti-mouse IgG (Sigma, 10 nm gold particle size). The small black spots indicate the presence of gold nanoparticles, and hence, the mouse α -VSV antibody.

The amphiphilic block – copolymer tested by us for producing the polymersomes is PBD-1200-PEO-600 (PolymerSource). This molecule consists of a hydrophobic poly(butadiene) domain conjugated to a hydrophilic poly(ethylene oxide) domain. The monoclonal rabbit antibody raised against poly-ethylene-glycol (α -PEG) is able to bind specifically to the hydrophilic poly(ethylene oxide) domain and is therefore suitable for this harvesting endeavor. The ability of α -PEG-modified SiNP to immunoprecipitate polymersomes was evaluated in two ways: First of all, phase-contrast microscopy was used to determine if pGUVs are co-localized with the anti-PEG antibody - SiNP forming an immunocomplex (Fig. 3A). As a second strategy to show the immunocomplex formation, fluorescent dye labelled polymersomes were used (see ESI). The polymersomic GUVs were sedimented at 600 x g for 1 min and treated with 100 mM NaOH for 10 min in order to release the polymersome – SiNP immunocomplex. Followed by another centrifugation step to separate the SiNPs and release pGUVs. The microscopical images in phase contrast mode present the polymersomes as individual spheres as the SiNPs are disconnected (Fig. 3B).

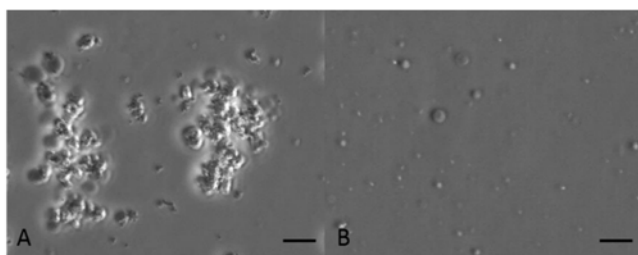


Fig. 3. A) Phase contrast micrograph showing pGUVs of several μm in size forming an immunocomplex with the smaller silica nanoparticles (SiNP) B) Micrograph showing released pGUVs present as individual, non-connected pGUVs after 100 mM NaOH treatment (scale bar; 10 μm).

Additionally, we present production and stabilization of unlabeled membrane protein species from various origins. In iMAPS, membrane proteins are reproducibly synthesized in the presence of polymeric membranes as a robust and chemically defined materials bypassing regulating mechanisms of a cell, but still implying the quality control and insertion mechanism of proteins, being processed in a cellular context. We present preparations in Fig. 4 from volume batches of 10 μl of cellular lysate (wheat germ) – for LHCII, this resulted in relatively high protein yields as shown in Fig. 4, for the human claudin 2, the synthesis level in the wheat germ extract was substantially lower but still reproducible and clearly detectable on a standard western blot. We could observe the polymeric matrix to stabilize the incorporated membrane protein species from protease degradation over several days up to weeks as we visualized pGUVs with LHCII proteins incorporated after several days, observing specific interactions of antibodies raised against an affinity tag of the protein by standard immunogold labelling procedure.

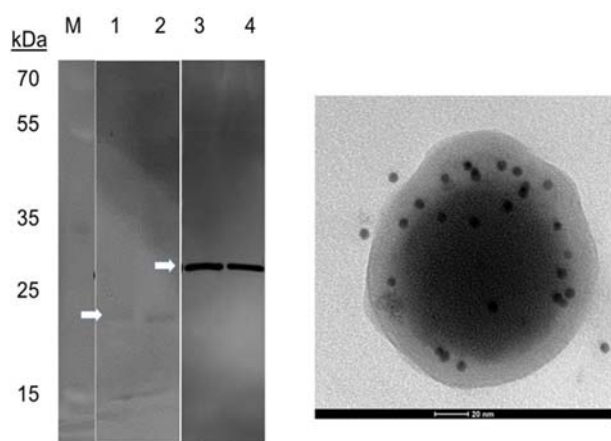


Fig. 4 On the left side: Examplic Western blot of immunoprecipitated LHCII proteopolymersomes containing the human claudin 2 (lane 1 and 2) and the plant protein LHCII in lane 3 and 4. Comparison between precipitation assay using a 'generic' polymer-specific antibody assay, namely α -PEG-functionalized SiNP versus a protein – specific ('non-generic') α -VSV-functionalized SiNP assay. The signals on the western blot indicate successful synthesis for both membrane protein species and sufficient interaction with the respective SiNP – functionalized antibodies. α -VSV-SiNP for sedimentation. Protein standard: PageRuler Plus Prestained Protein ladder. On the right side: Transmission electron microscope (TEM) image of an immunogold-labelled proteopolymersome with integrated light harvesting protein (LHCII). LHC functionalized immunoprecipitated proteopolymersomes were labelled by primary, monoclonal murine α -VSV antibodies secondary immunogold labelled anti-mouse IgG, followed by crosslinking within 2.5% glutaraldehyde and incubation in contrast agent, 1% OsO₄.

To determine if recovered antibody-modified SiNPs are able to repeatedly immunoprecipitate polymersomes, α -PEG-SiNPs were used to immunoprecipitate LHCII-proteopolymersomes in a 'recycling experiment' (Fig. 5). 5 μl polymersome preparations, functionalized by iMAPS into proteopolymersomes, were incubated for 1 h with 100 μg of α -PEG-modified SiNPs and incubated with overhead shaking at 60 rpm. The polymersome – SiNP complexes were then centrifuged at 1 700 x g for 5 min. The pelleted complexes were resuspended and incubated for 15 min with either 10 μl of 10 mM glycine/HCl pH 2 and alternatively 10 μl of 100 mM NaOH in order to release the immunocomplex between proteopolymersomes and SiNPs. After another centrifugation step the supernatants from each recovery process were analyzed using the standard Western blot immunodetection method while the SiNPs were reused. The respective blots showed successful immunoprecipitation after recycling of α -PEG-SiNPs (Fig. 5). The different LHCII signal intensities between the different rounds of recovery can be explained by batch to batch variations of LHCII expression efficiency, representing the very similar efficiency of the harvesting/release procedure. Optimal purification efficiency was achieved using an α -PEG-modified SiNP to polymersome ratio of 20:1, e.g. 100 μg of α -PEG-SiNP used for harvesting 5 μg of polymersomes. Both pH changes result in the efficient release of the immunocomplex as shown in the Fig. 5, demonstrating the efficiency of pH shift for the release of the desired proteopolymersomes after the harvesting procedure and - at the same time - enabled recycling of the antibody – functionalized SiNPs as the pH increase was moderate, and the antibodies did not lose their binding capacity.

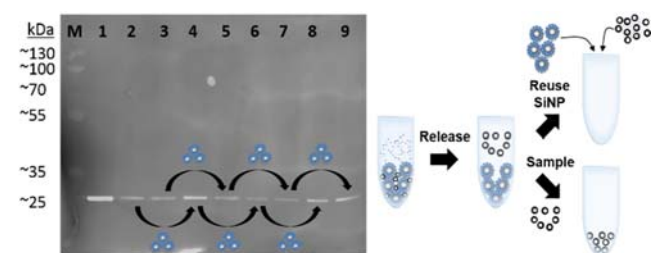


Fig. 5 Elution of polymersomes from α -PEG-SiNP and repeated use for immunoprecipitation based harvesting. α -PEG-SiNP were used to immunoprecipitate LHCII proteopolymersomes with integrated LHCII. The proteopolymersomes were then recovered using treatment with either 100 mM NaOH or 10 mM glycine/HCl. The recovered antibody-modified SiNP were then used two more times to immunoprecipitate LHCII proteopolymersomes. The supernatants from each recovery process were analyzed using Western blot. Lane M: PageRuler Plus Prestained Protein ladder. Lane 1: unpurified reaction mix containing LHCII produced in the absence of polymersomes. In lanes 2, 4, 6 and 8 elution with 10 mM glycine/HCl pH2 and successful reuse of the α -PEG-modified SiNP is shown. While in lanes 3, 5, 7 and 9, elution with 100 mM NaOH and reuse of the α -PEG-modified SiNP proved to be as successful as the acidic treatment.

The efficiency of our anti-PEG-SiNP-based immunoprecipitation method in order to purify LHCII proteopolymersomes was compared to the efficiency of centrifugal microfiltration. Both strategies are dependent on the use of polymersomes as robust matrices, hosting the protein of interest.

Centrifugal microfiltration has been described for the purification of proteopolymersomes from transcription-translation reaction mixtures.⁶ This method relies on the

membrane sieving of proteopolymersomes from the rest of the reaction mixture. For this to be effective, the diameter of the proteopolymersomes needs to be larger than the cut-off size of the filters used. However, it should be noted that polymersomes in the same dimensions as the filter pore sizes might deform and penetrate the filter pores and thus be lost in the collection procedure. Furthermore, the efficiency and efficiency of purification by centrifugal microfiltration is dependent on the amount and size distribution of the polymersome sample. The length of time required for complete filtration also depends on the volume of the respective sample. Furthermore, localized concentration of polymersomes at the filter surface would result in blockage and severely reduce efficiency of contaminant removal.

Western blotting and staining of total protein content in a Coomassie stained – polyacrylamide gel electrophoresis (PAGE), indicated increased purification efficiency by the SiNP-based immunoprecipitation strategy (Fig. 6) versus the microfiltration – based purification procedure. Employing centrifugal microfiltration, we observed comparable amounts of background protein levels but much lower LHCII levels. The centrifugal microfiltration strategy resulted in only approximately 7% of the immunoprecipitation method, which can be considered as a trade – off for the circumstance, that neither any antibody material nor any nanoparticles have to be involved in the microfiltration procedure but a standard AMICON® filter.

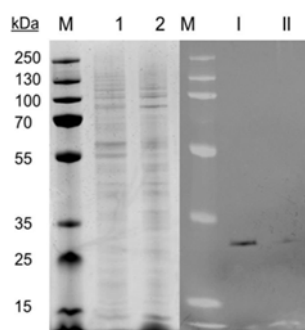


Fig. 6 Coomassie staining and immunoblotting experiment of Proteopolymersomes, purified via centrifugal microfiltration versus α -PEG-modified SiNP immunoprecipitation. Lane M appears twice and represents the protein standard in apparent molecular weights, indicated in kDa. All sample lanes contain the result of a 10 μ l transcription-translation reaction mixture with cDNA coding for the LHCII protein. After purification via immunoprecipitation, employing α -PEG-modified SiNP, each sample was exposed to a standard gel electrophoresis (PAGE), followed by Coomassie staining. Lane 1 represent the sample experiencing immunoprecipitation, Lane 2 represent total protein staining after microfiltration – based purification. Lane I and II present the respective samples transferred onto a nylon membrane and exposed to an immunoblotting experiment.

The presented SiNPs-based immunoprecipitation method renders a straight forward approach for membrane protein synthesis and isolation of membrane proteins combined by a one-step purification procedure with the SiNPs involved reversibly forming an immunocomplex allowing for regeneration of the antibody – functionalized SiNPs for effective harvesting. The procedure is applicable for any membrane protein species with known cDNA sequence. The use of an antibody that targets the material of the polymeric membrane material, rather than the membrane proteins

also allows membrane protein purification even if a specific antibody is not available. Furthermore the optimal purification and release conditions need to be adjusted just once and not for every monoclonal antibody raised against the protein of interest. The membrane protein of interest in the polymersomal matrix appears secured in chemically defined and robust proteopolymersomes. Subsequent elution from the SiNPs yields intact proteopolymersomes that may be used for vaccination or – as a perspective for the emerging field of membrane protein-related device fabrication – in robust, polymeric surfaces presenting membrane proteins for sensing and actuating.

Acknowledgements

We thank the Ministry of Transportation and Innovation, BMVIT, Austria, for financial support of the International Graduate School, IGS. We cordially thank Prof. Harald Paulsen, University of Mainz, Germany, for kindly providing the cDNA of LHCII and the chlorophyll preparation.

Notes and references

- 1 S. Kalipatnapu and A. Chattopadhyay, *IUBMB Life*, 2005, **57**, 505–512.
- 2 H. Rogl, K. Kosemund, W. Kühlbrandt and I. Collinson, *FEBS Lett.*, 1998, **432**, 21–26.
- 3 A. M. Seddon, P. Curnow and P. J. Booth, *Biochim. Biophys. Acta BBA - Biomembr.*, 2004, **1666**, 105–117.
- 4 R. Sachse, S. K. Dondapati, S. F. Fenz, T. Schmidt and S. Kubick, *FEBS Lett.*, 2014, **588**, 2774–2781.
- 5 N. Shadiac, Y. Nagarajan, S. Waters and M. Hrmova, *Mol. Membr. Biol.*, 2013, **30**, 229–245.
- 6 M. Nallani, M. Andreasson-Ochsner, C.-W. D. Tan, E.-K. Sinner, Y. Wisantoso, S. Geifman-Shochat and W. Hunziker, *Biointerphases*, 2011, **6**, 153–157.
- 7 M. Antonietti and S. Förster, *Adv. Mater.*, 2003, **15**, 1323–1333.
- 8 B. M. Discher, Y. Y. Won, D. S. Ege, J. C. Lee, F. S. Bates, D. E. Discher and D. A. Hammer, *Science*, 1999, **284**, 1143–1146.
- 9 R. Rodríguez-García, M. Mell, I. López-Montero, J. Netzel, T. Hellweg and F. Monroy, *Soft Matter*, 2011, **7**, 1532–1542.
- 10 D. Basu, J. M. Castellano, N. Thomas and R. K. Mishra, *Biotechnol. Prog.*, 2013, **29**, 601–608.
- 11 J. S. Lee and J. Feijen, *J. Controlled Release*, 2012, **161**, 473–483.
- 12 H. Bermudez, A. K. Brannan, D. A. Hammer, F. S. Bates and D. E. Discher, *Molecular Weight Dependence of Polymersome Membrane Structure, Elasticity, and Stability*, 2002.
- 13 WO/2014/077781, 2014.
- 14 T. Kobayashi, S. Mikami, S. Yokoyama and H. Imataka, *J. Virol. Methods*, 2007, **142**, 182–188.
- 15 A. Nozawa, T. Ogasawara, S. Matsunaga, T. Iwasaki, T. Sawasaki and Y. Endo, *BMC Biotechnol.*, 2011, **11**, 35.
- 16 M. A. Goren and B. G. Fox, *Protein Expr. Purif.*, 2008, **62**, 171–178.
- 17 R. E. Lane, D. Korbie, W. Anderson, R. Vaidyanathan and M. Trau, *Sci. Rep.*, 2015, **5**.
- 18 T. Genji, A. Nozawa and Y. Tozawa, *Biochem. Biophys. Res. Commun.*, 2010, **400**, 638–642.

- 19 T. Kawate and E. Gouaux, *Struct. Lond. Engl.* 1993, 2006, **14**, 673–681.
- 20 W. Stöber, A. Fink and E. Bohn, *J. Colloid Interface Sci.*, 1968, **26**, 62–69.
- 21 D. Christensen, C. Foged, I. Rosenkrands, H. M. Nielsen, P. Andersen and E. M. Agger, *Biochim. Biophys. Acta*, 2007, **1768**, 2120–2129.

Supporting Information for:

Nanoscopic Harvesting of Polymeric – stabilized Membrane Proteins

Thomas Zapf^a, Christian Zafiu^b, Christoph Zaba^a, Chong-Wen Darren Tan^a, Walter Hunziker^c and Eva-Kathrin Sinner^a

^a Department for Nanobiotechnology
Institute of Synthetic Bioarchitectures
University of Natural Resources and Life Science
Muthgasse 11/2, 1190 Vienna, Austria

^b ICS-6 Structure Biochemistry
Forschungszentrum Jülich
Wilhelm-Johnen-Straße, 52425 Jülich, Germany

^c Institute of Molecular and Cell Biology
A*Star, Singapore
61 Biopolis Drive, Proteos, 138673 Singapore

E-mail: eva.sinner@boku.ac.at

Experimental Section

Silica nanoparticle formation

Silica nanoparticle formation was based on the Stöber process.¹ For the production of 50 ml of 550 nm sized silica nanoparticles (SiNPs), 3.13 ml of tetraethyl orthosilicate (98%, Sigma-

Aldrich), 10.61 ml ultrapure water, 2.9 ml ammonium hydroxide (30-33%, Sigma-Aldrich) and 33.36 ml ethanol (96%, Merck) were mixed in a one-step reaction. The mixture was rigorously stirred with a magnetic stirrer for 4 hours within a sealed bottle to prevent evaporation of the solvent and changes to the chemical composition. The reaction mix was then centrifuged at 1 700 x g for 10 min and the pellet was washed by resuspension and centrifugation three times with ethanol and three times with ultrapure water before drying under vacuum under the same centrifugation parameters as before. The size of the resultant nanoparticles was dependent on the amount of ammonia present in the solution.

All incubations were performed at room temperature unless stated otherwise. If not stated otherwise, centrifugation condition is 1 700 x g for 5 min.

Surface modification of SiNPs

10 mg of dry SiNPs were taken up in 1 ml of 96% ethanol, sonicated until the SiNPs were dissolved (37 kHz and 80 W) and then centrifuged. All centrifugation steps in this following procedure was performed at 1 700 x g for 5 min. The pellet was resuspended in 950 μ l of 96% ethanol and 50 μ l of (3-aminopropyl) triethoxysilane (APTES) (99%, Sigma-Aldrich) followed by 14–16 h incubation on an overhead shaker at 60 rpm. The SiNPs were centrifuged again and washed with 1 ml ethanol to remove excess APTES. The nanoparticles were resuspended in 1 ml of ultrapure water and stored at 4°C until further usage at a particle concentration of 10 mg/ml.

For the coupling of antibodies to the nanoparticle surface, 100 μ l of the amino-functionalized SiNPs solution were pelleted by centrifugation and subsequently resuspended in 500 μ l of ultrapure water containing 0.4 M 1-ethyl-3-(3-dimethylaminopropyl) carbodiimide (EDC) (\geq 99%, Roth) and 0.1 M N-hydroxysuccinimide (NHS) (98%, Sigma) and incubated on an overhead shaker for 10 min before being centrifuged again at 1 700 x g for 5 min. Supernatant was discarded and the pellet was resuspended by sonication in 1 ml of 10 mM Glycine (\geq 99%, Promega)/HCl (Roth) pH 5 containing 1 μ g of antibody, either monoclonal rabbit anti-polyethylene-glycol (α -PEG)(C/N: ab51257, ABCAM) or monoclonal mouse anti-vesicular stomatitis virus G (α -VSV) (C/N: V.5507, Sigma-Aldrich), respectively. The combination of SiNPs with the respective antibody was incubated for 1 h on an overhead shaker at 60 rpm before pelleting by centrifugation 1700 x g for 5 min. The SiNPs were then resuspended in 1 ml of 1 M ethanolamine (\geq 99%, Roth) and incubated for 10 min to deactivate any residual activated carboxyl groups. After centrifugation and pelleting, the SiNP were resuspended repetitively with ultrapure water to wash away residual ethanolamine. The pelleted SiNPs were

finally resuspended in 100 µl of phosphate-buffered saline (PBS) resulting in a final concentration of 1 mg per 100 µl antibody-conjugated SiNPs and stored at 4°C until further usage.

DLS and Zeta potential measurement before and after SiNP surface modification

Modification of the silica surface was monitored by measurements of dynamic light scattering (DLS) and zeta potential with the Zetasizer device (Malvern Instruments, Zetasizer Nano-ZS) (Fig. 1S). The measurements were performed in ultrapure water as well as 96% ethanol at a concentration of 1 mg/ml of SiNPs. Three analyses with multiple runs (18 for DLS, 12 for zeta potential) were performed. The DLS measurements were made within disposable microcuvettes (Roth, $z = 8,5$ mm) while for zeta potential measurements disposable zeta potential cells (DTS 1060/1070) were used.

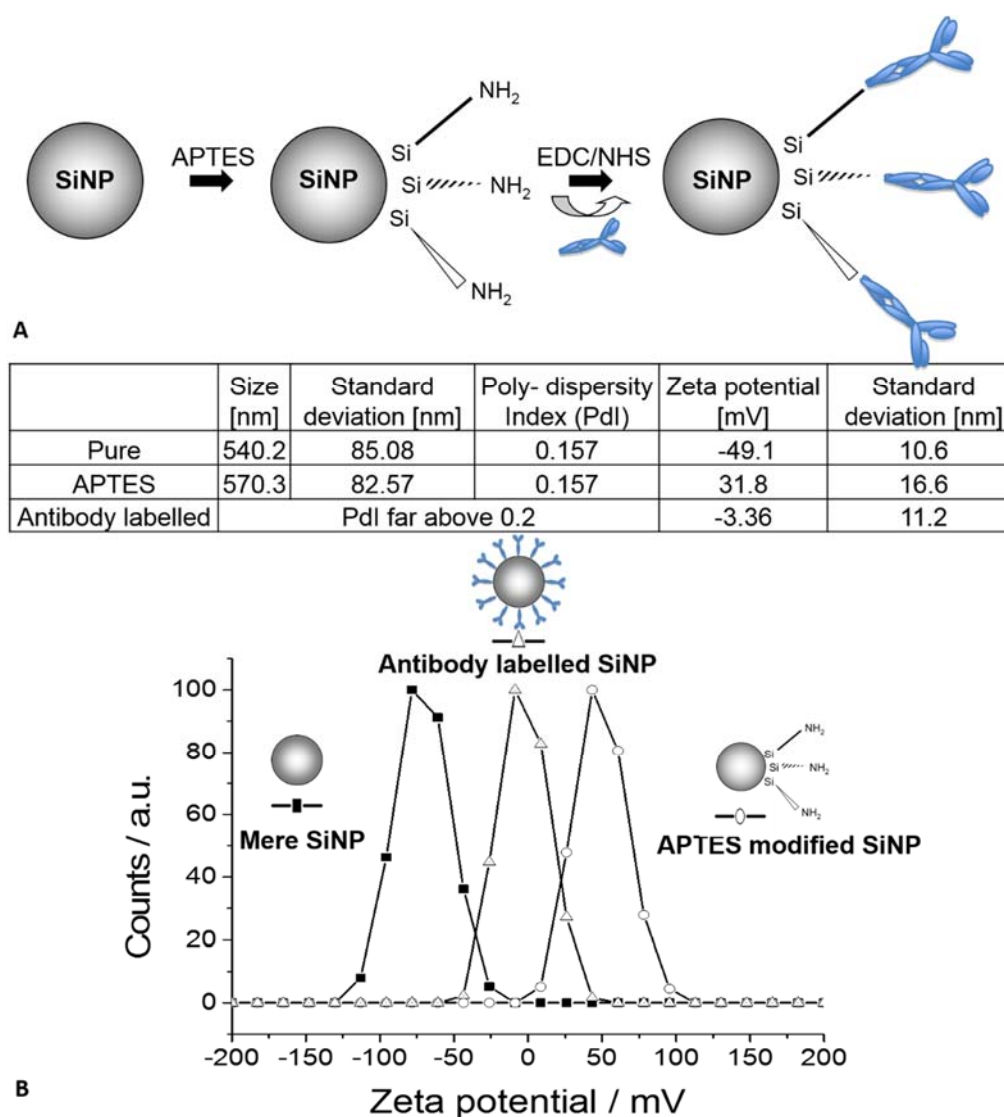


Fig. 15 A) Schematic overview of the SiNP modification. B) DLS and Zeta potential measurement profiles demonstrate that DLS and Zeta potential measurement can be successfully used to monitor the surface modification.

Visualization of SiNP surface modification by transmission electron microscopy (TEM)

Briefly, 10 μg (corresponding in ca. 10 μl sample volume) of α -VSV-modified SiNPs were incubated in 1 ml PBS with 1 $\mu\text{g}/\text{ml}$ immunogold-labelled goat anti-mouse IgG (C/N: G7777, Sigma, 10 nm gold particle size) for 1 hour prior to centrifugation for 5 min at 1 700 x g. One centrifugal washing step in 1 ml PBS (5 min at 1 700 x g) was performed to get rid of residual unbound goat anti-mouse IgG before resuspension in 10 μl of PBS was performed. The suspension was adsorbed for 15 min on a TEM copper grid. Residual suspension was subsequently removed and the grid was dried in air over night at room temperature before analysis.

Visualization of LHCII in polymersomes by transmission electron microscopy (TEM)

For transmission electron microscopy (TEM), LHCII proteopolymersomes, synthesized with 0.4 M trehalose, were prepared as described later and immunogold-labelled using rabbit anti-LHCII antibodies (1 µg/ml in Carl Roth Roti®-Block, Mainz, Harald Paulsen) as the primary antibody and immunogold-labelled goat anti-rabbit antibody (5 nm colloidal gold, Sigma, 1:100 diluted in Roti®-Block, Carl Roth) as the secondary antibody. The incubation and blocking of the TEM grids was done in a similar manner as Western blotting described later. Antibody incubation times were reduced to 30 min each, followed by 15 min of 2.5% glutaraldehyde fixation. For the staining of the polymersome membranes 1 h incubation with 1% OsO₄ and three subsequent washing steps in ultrapure water were performed.

Formation of polymersomes and chloroplast-pigment extract-containing polymersomes

The polymer poly(butadiene) (PBD₁₂₀₀-PEO₆₀₀, PolymerSource) was either dissolved as is or for identification of presence of polymersomes, incubated in crude total pigment extract derived from peas, at a pigment to polymer molar ratio of 1:200, in chloroform (≥99%, Roth). Crude total pigment was extracted from peas as described by Paulsen et al.² Aliquots of each chlorophyll preparation were dried into a thin pigment-polymer film in a glass round-bottom flask using a rotary evaporator and subsequently rehydrated in ultrapure water to a final concentration of 5 mg/ml. Each rehydration was subjected to five freeze-thaw cycles using a liquid nitrogen bath as well as an ultrasonic waterbath at 37°C in order to form unilamellar polymersomes³. For a uniform size distribution, the polymersomes were extruded 20 times through a 200 nm membrane filter (polycarbonate, 0.75'', AVESTIN) and characterized using DLS and transmission electron microscopy (TEM).

Polymersomic Giant Unilaminar Vesicles (GUVs) were formed from poly(butadiene) in 0.4 M sucrose (≥99.5%, Roth) at 37°C with the Nanji[on Vesicle Prep Pro® chamber at a frequency of 5 Hz, amplitude of 3 V, a rise time of 1 min, main time of 120 min and a fall time of 5 min.

Fluorescence of pigmented polymersomes was analyzed with the Luminescence Spectrometer (LS 55, PerkinElmer Instr.) using disposable microcuvettes (Roth, z = 8,5 mm). Chlorophyll fluorescence was excited at wavelengths from 350 nm to 480 nm while fluorescence emission was recorded at 670 nm. This wavelength correlates to the maximal fluorescence of chlorophyll a that had been integrated into the membrane of the polymersomes, as the major component of the added pigment extract.

Synthesis of the exemplar membrane protein species and formation of proteopolymersomes

To demonstrate the efficacy of our method of immunoprecipitation, we aimed to purify polymersomes with embedded membrane proteins. Respective cDNA with the coding sequence for an N-terminal Vesicular stomatitis virus glycoprotein (VSV) were used in the coupled transcription and translation system from wheat germ: The TNT® Quick Coupled Transcription/Translation system (L4140, Promega) was employed to express the pea derived (*Pisum sativum*) Light Harvesting Complex II (LHCII) under regulation of a T7 promoter. The reaction mix of a total volume of 10 µl were composed according to the suppliers instructions, however, the suppliers recommendation advises for 25 – 50 µl total volume, whereas in our hands, 10 µl was sufficient for the immunoprecipitation methods, resulting in ca. 200 ng of desired protein, visualized by western blotting experiments. For the formation of proteopolymersomes, 2 µg of polymersomes (average size 200 nm) was added to 10 µl of reaction mix for co-translational insertion of the LHCII into the polymer membrane. The preparations were then incubated for 90 min at 30 °C and shaken at 350 rpm. The final proteopolymersome/cell lysate sample was either stored at 4 °C up to several weeks or directly processed by microfiltration/immunoprecipitation for purification.

Electrophoresis and Western blot analyses

All samples for electrophoresis were diluted 1:1 with 2 x NuPAGE® (Life Technologies) gel loading buffer (prepared from NuPAGE® LDS Sample Buffer (4x) and NuPAGE® Reducing Agent (10x)) and incubated at 70 °C for 10 min. Each was then loaded into a 10% NuPAGE® Bis-Tris gel and reducing sodium dodecyl sulfate-polyacrylamide gel electrophoresis (SDS-PAGE) was performed using the MOPS NuPAGE® SDS Running Buffer at a constant voltage of 200 V and 400 mA for 55 min.

Protein in the Bis-Tris gel was transferred to a nitrocellulose membrane using the iBlot™ System (Invitrogen) at 20 V for 7 min. The membrane was blocked for 1 h with gentle agitation using Odyssey™ Blocking Buffer, then incubated for 1 h with gentle agitation with monoclonal mouse anti-vesicular stomatitis virus G (α-VSV) (C/N: V.5507, Sigma-Aldrich) diluted 1:10 000 in Odyssey™ Blocking Buffer. This was followed by washing of the membrane with PBS supplemented with 0.01% Tween 20® (PBST) for 5 min. This was repeated 4 more times. Subsequently, infra-red dye-labeled goat anti-mouse IgG (C/N: 926-68021, IRDye 800CW, LI-COR Biosciences) was diluted 1:10 000 in a mixture of Odyssey™ Blocking Buffer diluted with PBS at a ratio of 1:1. The membrane was incubated for another 1 h with gentle agitation.

Finally, the membrane was washed three times with PBST and twice with PBS. Once the membrane was completely dried, it was scanned using the Odyssey™ CLx infrared system (LI-COR Biosciences).

Immunoprecipitation of pigmented polymersomes and polymersomic GUVs

We validated the harvesting steps on microscopical scale using conventional phase contrast light microscopy of polymersomes interacting with α -PEG-SiNPs as 'anchoring' structures. Briefly, 100 μ g of α -PEG-SiNPs were incubated with GUVs in 1 ml of PBS and incubated on an overhead shaker at 60 rpm for 1 h, followed by centrifugation at 600 x g for 1 min. The resulting pellet was gently resuspended in 20 μ l of ultrapure water and 5 μ l was used for microscopy. From the images, we learned that a strong connecting network from the SiNP had been formed, interconnecting the large polymersomes.

To evaluate the efficiency of immunoprecipitation using antibodies targeting polyethylene glycol the polymer membrane, 5 μ g of 200 nm-sized pigment-containing polymersomes were diluted with 1 ml of PBS and incubated with 0, 10, 25, 50, 75, 100 and 125 μ g of α -PEG-modified SiNPs for 1 h on an overhead shaker. After centrifugation for 5 min at 1, 700 x g the supernatant was collected and analyzed for chlorophyll fluorescence. The data (Fig. 2S/A) indicates maximal supernatant fluorescence in absence α -PEG-SiNP. However, taking different samples with increased amounts of α -PEG SiNPs material, harvesting the polymersomes resulted in a decrease of fluorescence. Quantities of α -PEG-SiNP greater than 50 μ g did not result in further reduction of fluorescence. This observation indicates a clearance of the pigmented polymersomes from the supernatant by the α -PEG-SiNP immunocomplex formation.

In case of polymersomic GUVs release the formed immunocomplex was sedimented at 600 x g for 1 min, supernatant discarded and the pellet treated with 20 μ l 100 mM NaOH for 10 min in order to release the polymersome – SiNP immunocomplex. Subsequent centrifugation at 600 x g for 1 min was done to separate GUVs and SiNPs.

In case of fluorescent labelled polymersomes the sediment of each pigmented polymersome-SiNP clusters was resuspended in 100 μ l of 10 mM NaOH ($\geq 99\%$, Gerbu) for 10 min and centrifuged again. The supernatant was collected and analyzed for chlorophyll fluorescence. We observed substantial increase of fluorescence as a function of releasing the polymersomes from the SiNPs back into the bulk phase. Figure 2S/B depicts the fluorescence

measurements of the very same samples, employed for the fluorescence decrease in the supernatant as function of SiNP – polymersome complex formation, shown in Fig. 2 S/B.

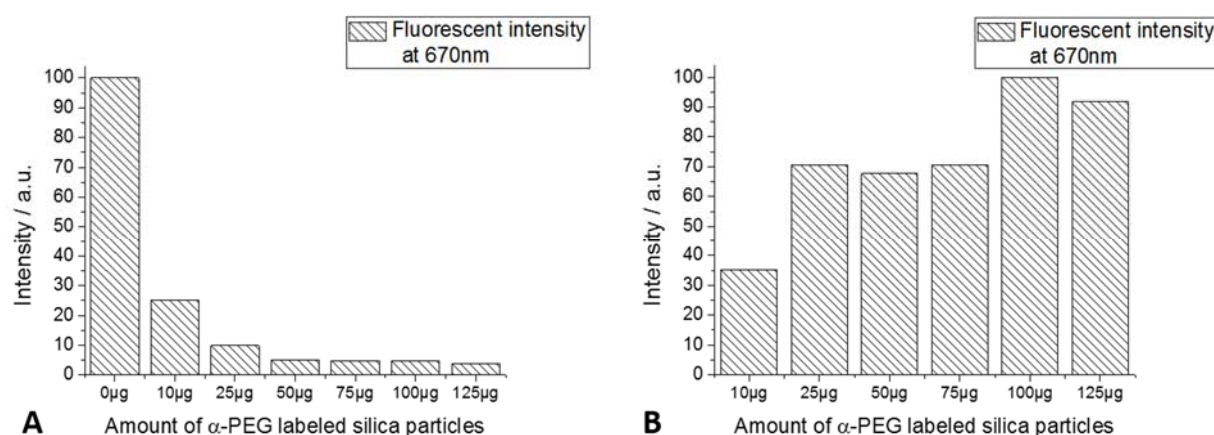


Fig. 2S A) Fluorescence analyses of supernatant after immunoprecipitation of pigmented polymersomes. Different amounts of α -PEG-SiNP were tested for their efficiency in immunoprecipitating 5 μ g of 200 nm pigmented polymersomes. Fluorescence was normalized against the sample set maximum and indicates the presence of pigmented polymersomes. Analysis of the supernatants following immunoprecipitation shows a decrease in fluorescence at 670 nm with an increase in the amount of α -PEG-SiNP used. B) Fluorescence signals of chlorophylls, embedded in polymersome matrix after pH increase.

Immunoprecipitation of proteins and proteopolymersomes and reusability of antibody – functionalized SiNPs

Proteopolymersomes produced in transcription-translation reaction mixtures of 10 – 20 μ l were first incubated for 1 h with 100 μ g of α -PEG-modified SiNPs for each 5 μ g of polymersomes and incubated with overhead shaking at 60 rpm. The mixtures were then centrifuged at 1 700 x g for 5 min and the pellets were used directly for electrophoresis. Alternatively, the pellet was resuspended and incubated for 15 min with either 10 μ l of 10 mM glycine/HCl pH 2 or 10 μ l of 100 mM NaOH to release the antibody-bound LHCII and Cldn2 proteopolymersomes. The supernatants were further treated for 1 h as described above with α -VSV-modified SiNPs. This allowed us to capture LHCII and Cldn2 that had not integrated into the polymersome membranes. In case of Cldn2, after SiNP based polymersome removal, Tween 20® (Sigma-Aldrich) had to be added to the supernatant up to a final concentration of 0.1% Tween 20® in order for the non-integrated protein to be immunoprecipitated. The samples were centrifuged

again at 1 700 x g for 5 min and the pellets were used directly for electrophoresis. Furthermore, the reusability of the SiNP after 10 mM glycine/HCl pH 2 or 10 µl of 100 mM NaOH was tested.

Testing of unlabeled APTES-modified SiNP resulted into no detectable immunoprecipitation with of proteopolymersomes with the SiNPs.

To determine if recovered antibody-modified SiNPs are still able to immunoprecipitate polymersomes, α-PEG-SiNPs were used to immunoprecipitate LHCII-proteopolymersomes. The proteopolymersomes were recovered dissolving the immunocomplex with either 100 mM NaOH or 10 mM glycine/HCl. The recovered antibody-modified SiNPs were then used two more times to immunoprecipitate LHCII-proteopolymersomes. The supernatants from each recovery process were analyzed using the standard Western blot.

Comparison of centrifugal microfiltration and immunoprecipitation for proteopolymersome purification

For Amicon® centrifugal microfiltration 10 µl of transcription-translation reaction mixture containing 5 µg of LHCII proteopolymersomes were diluted with 500 µl of PBS, then loaded into an Amicon® centrifugal microfiltration cartridge (Ultrafree®-MC-VV, Durapore® PVDF 0.1µm). The samples were then centrifuged at 600 x g until all the solution had filtered through the cartridge. The retentates were resuspended in 20 µl PBS.

For antibody-modified SiNP immunoprecipitation 10 µl of transcription-translation reaction mixture containing 5 µg of LHCII proteopolymersomes were treated with 100 µg of α-PEG-SiNPs in 1 ml of PBS. The mixtures were incubated on an overhead shaker at 60 rpm for 1 h, then centrifuged at 1 700 x g for 5 min. The pellets were resuspended in 20 µl PBS.

Samples prepared using both methods of purification were denatured and electrophoresed as described above. Subsequently, the Bis-Tris gels were removed from the plastic casing and rinsed for 5 min in deionised water. The water was then replaced with 20 ml of SimplyBlue™ SaferStain for total protein staining and the gel was incubated for 1 h with gentle agitation. The SimplyBlue™ SaferStain was replaced with deionised water and the gel was again incubated for 1 h with gentle agitation. A final rinsing with deionised water was performed before the gel was scanned using the Odyssey™ CLx infrared system. Alternatively, the proteins in the gel were blotted onto nitrocellulose membranes and analyzed by Western blot, as described above.

References

- 1 W. Stöber, A. Fink and E. Bohn, *J. Colloid Interface Sci.*, 1968, **26**, 62–69.
- 2 H. Paulsen, U. Rümmler and W. Rüdiger, *Planta*, 1990, **181**, 204–211.
- 3 M. Traïkia, D. E. Warschawski, M. Recouvreur, J. Cartaud and P. F. Devaux, *Eur. Biophys. J. EBJ*, 2000, **29**, 184–195.

2.2. Functional Synthesis of the Light Harvesting Complex II into Polymeric Membrane Architectures

Authors:

Thomas Zapf, Darren Tan Chong-Wen, Tobias Reinelt, Christoph Huber, Ding Shaohua, Susana Geifman-Shochat, Harald Paulsen, Eva-Kathrin Sinner

Journal:

Angewandte Chemie International Edition, 2015

Received: 08 Jul 2015

Revised: 28 Jul 2015

Accepted: 06 Aug 2015

DOI: 10.1002/anie.201506304

Motivation:

The light-harvesting complex II (LHCII) of higher plants belongs to the best studied membrane proteins. LHCII's intrinsic chlorophyll and carotenoid binding properties displays a highly interesting feature for potential sensor and photovoltaic purposes. The process of light harvesting is a highly conserved process found in organisms ranging from simple *Archea* to plants. Throughout evolution the core structure and function of the light harvesting complex has remained highly conserved.

LHCII has been functionally reconstituted into lipid membranes from plant derived extracts⁷ as well as after being recombinantly expressed within *E.coli*⁸. Even the successful co-translational cell-free expression into lipid vesicles was previously achieved.⁷⁷ Nevertheless lipid bilayers are prone to oxidation and are relatively unstable for long term usage. We exchange lipid membranes through the usage of an amphiphilic diblock copolymer species to create a more stable environment.

Through the usage of a cell-free system, in our case a wheat germ based plant extract, supplemented with polymeric membrane supports, we tried to mimic the process occurring *in situ* upon LHCII insertion into the thylakoid membrane. We aimed for the functional insertion of LHCII-pigment complexes into polymeric membranes, both vesicular and planar structures. Orientation of insertion as well as functionality, in case of LHCII - binding and arrangement of chlorophylls and carotenoids - were the subject of investigation.

In the case of planar tethered polymer bilayers integrated with LHCII-pigment complexes, the integration and resulting functionality were investigated using Surface Plasmon Resonance (SPR) and Surface Plasmon enhanced Fluorescence Spectroscopy (SPFS). Reliability of LHCII function was observed by taking advantage of the phenomena that on the one side surface plasmons are able to excite fluorophores through their evanescence field as well as the fact that successful energy transfer from *Chl b* to *Chl a* has shown to be a reliable indication of LHCII functionality⁸.

Synthesis and Functional Reconstitution of Light-Harvesting Complex II into Polymeric Membrane Architectures

Thomas Zapf[a] MSc, Dr. Darren Tan Cherng-Wen[a], Tobias Reinelt[a], Dr. Christoph Huber[a], Dr. Ding Shaohua[b], Prof. Dr. Susana Geifman-Shochat[c], Prof. Dr. Harald Paulsen[d], Prof. Dr. Eva-Kathrin Sinner[a]*

DOI: 10.1002/anie.201506304

One of nature's most effective evolutionary concepts is the harvesting and dissipation of solar energy comprised with the help of light harvesting complex II (LHCII). This protein, along with associated pigments is the main solar energy collector in higher plants. We aimed to generate stable, highly controllable and sustainable polymer-based membrane systems containing LHCII-pigment complexes ready for light harvesting. LHCII was produced by cell-free protein synthesis based on wheat-germ extract, and the successful integration of LHCII and its pigments into different membrane architectures was monitored. The unidirectionality of LHCII insertion was investigated by protease digestion assays. Fluorescence measurements indicated chlorophyll integration in the presence of LHCII in spherical as well as planar bilayer architectures. Surface plasmon enhanced fluorescence spectroscopy (SPFS) was used to reveal energy transfer from *chlorophyll b* to *chlorophyll a*, which indicates native folding of the LHCII proteins.

Light harvesting complex II (LHCII) of higher plants is one of the most abundant membrane proteins in the world. One LHCII protein can bind 14 chlorophylls (eight *Chl a*, six *Chl b*) and 4 carotenoids.^[1] LHCII serves as an antenna complex and is one of the few membrane protein species that can be spontaneously refolded *in vitro*, however, it tends to insert into membrane architectures with random orientation.^[2–4] LHC II is an attractive choice for the use in membrane protein research, and it has potential biotechnological importance as a pigment “organizer” in the context of sustainable, robust and efficient solar cells exists^[5]. So far approaches in LHCII research are dependent on reconstitution of the purified protein in detergents, amphiphiles

and lipid membranes.^[6,7]

Cell-free expression in systems supplied with artificial membranes, also referred to as *in vitro* membrane-assisted protein synthesis (iMAPS), offers a robust and reliable technique for the *de novo* synthesis of membrane proteins in artificial membrane supports, as has been shown for GPCRs^[8] claudin-2,^[9] and others.^[10,11] Recent attempts to replace lipid membranes by polymeric membrane mimics offers an interesting alternative since polymeric membranes produce reproducible and robust alternative membrane architectures.^[12] We selected polymeric membrane mimics from amphiphilic diblock copolymers, which assemble into bilayered membrane structures in aqueous environments.^[12–14] The polymer membrane architectures are easily tunable in terms of thickness, permeability and rigidity through selection of different polymers.^[14] The use of cell-free protein production allows *de novo* synthesis of membrane proteins in membranes, while bypassing potentially limiting cellular regulatory mechanisms and the bottleneck of purification through detergent induced denaturation.^[9,11,15,16]

Herein we show the functional and unidirectional insertion of LHCII and LHCII-pigment complexes into spherical polymersomes and planar polymer bilayers. Cell-free protein synthesis provides co-translational, unidirectional membrane protein insertion into polymeric membrane structures, as we described previously.^[9] We monitored the self-assembling of thiolated lipoic acid tethered polymeric membranes on planar gold substrates followed by integration of LHCII by iMAPS from wheat-germ-based cell-free lysates. Surface plasmon resonance (SPR) spectroscopy was used to monitor membrane formation, whereas energy transfer from *Chl b* to *Chl a* was observed by surface plasmon enhanced fluorescence spectroscopy (SPFS). Successful energy transfer following *Chl b* excitation by the evanescent plasmon field indicates native folding of LHCII moieties in the polymeric membranes and functional presentation of the chlorophyll molecules.

The synthesis of LHCII apoprotein and its integration into polymeric membranes was achieved through wheat-germ-based cell-free protein synthesis (Promega, L4140) as a suitable cell lysate system for plant proteins. The influence of polymersome concentration on the protein yield of N- and C- terminal VSVG tagged LHCII was assessed by using SDS-PAGE followed by Western blotting (Figure 1A). We observed stable LHCII expression levels up to a concentration of 0.5µg/µl polymer material (Figure 1B). We hypothesize that the optimal polymersome versus cell lysate ratio can be interpreted as being the result of molecular crowding, which is known to increase the robustness of cell-free gene expression.^[17] The surface to

[a] T. Zapf, CW. D. Tan, T. Reinelt, C. Huber, EK. Sinner
Department for Nanobiotechnology
Institute of Synthetic Bioarchitectures
University of Natural Resources and Life Science
Muthgasse 11/2, 1190 Vienna, Austria
E-mail: eva.sinner@boku.ac.at

[b] D. Shaohua
CAS Key Lab of Bio-Medical Diagnostics
Suzhou Institute of Biomedical Engineering and Technology,
Chinese Academy of Sciences
Keling Road 88, 215163 Suzhou, China

[c] S. Geifman-Shochat
School of Biological Science
Nanyang Technological University, Singapore
60 Nanyang Drive, 637551 Singapore, Singapore

[d] H. Paulsen
Institute of General Botany
Johannes Gutenberg University Mainz
Johannes-von-Müller-Weg 6, 55128 Mainz, Germany

Supporting information for this article is given via a link at the end of the document

volume ratio also plays a role, as we have demonstrated in a microfluidic system.^[18]

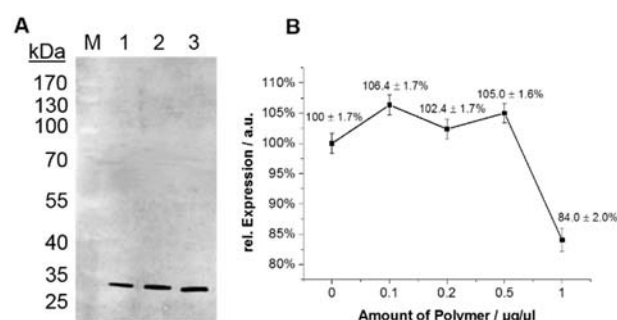


Figure 1. Expression of LHCII in the presence of polymersomes. A) Western blot of LHCII in the presence and absence of polymersomes. Lane 1 shows the expression of N-VSVG tagged LHCII alone. Lane 2 shows the N-VSVG tagged LHCII with 0.2 μg/μl polymersomes and Lane 3 shows the equivalent synthesis with C-VSVG tagged LHCII. B) The dependence of relative protein expression (as represented by signal intensity (n=3)) on polymer concentration.

Transmission electron microscopy (TEM) was performed to visualize presence, organization, amount and localization of LHCII protein moieties. Polymersomes with incorporated LHCII so called Proteopolymersomes (PPs), were purified as described by Nallani *et al.*^[9] The resulting PPs were stained by two different methods: 1) Membrane and protein staining with 1% Uranyl acetate and subsequent 1% OsO₄ (Figure 2A), as well as immunostaining with gold labeled anti-LHCII antibodies, and 2) staining with 1% OsO₄, thereby rendering the LHCII protein moieties as light spots (see Figure 2 B). For both preparation methods, the polymersomes tended to deform slightly during sample preparation. To minimize this effect, we loaded the polymersomes with 0.4 M trehalose, which is an established method for increasing stability.^[19]

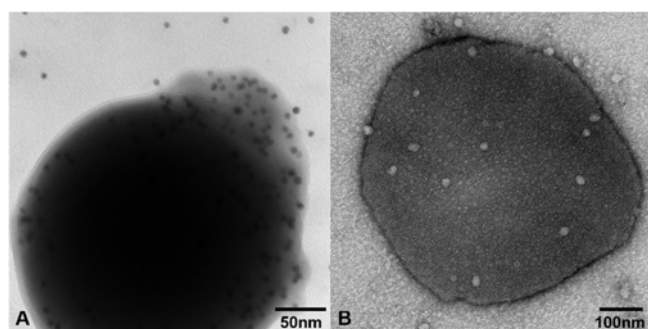


Figure 2. Transmission electron micrographs of LHCII-PPs purified by centrifugal ultrafiltration. A) Spherical polymersome containing immunogold-labelled LHCII. B) A polymersome after treatment with OsO₄; the white marks indicate unstained LHCII protein molecules.

Integration of LHCII into the polymersomes was confirmed using purification with a combination of immunoprecipitation^[20] and sodium carbonate extraction as described by Fujiki *et al.*,^[21] with minor adaptations and modifications (see the Supporting Information). According to this method, a highly ionic buffer disrupts simple adsorption of proteins to the polymersome membrane surface, and thus extracts partially embedded proteins. However proteins that are properly integrated into the membrane plane would be resistant to extraction. Our

polymersomes were purified by using anti-polyethylene glycol (α-PEG) antibody immobilized onto silica nanoparticles (SiNP) as described previously by our group,^[20] which allows integrated LHCII to be separated from components of the cell lysate. This is possible because the α-PEG antibody is able to bind to the poly(ethylene oxide) part of the polymer. Figure 3 shows an example result, where the sodium carbonate treated samples indicate that iMAPS-generate LHCII is fully incorporated into the polymeric membrane. The specific signal indicates the presence of LHCII as an integral membrane protein. Loss of signal strength is caused by the additional carbonate treatment. The antibody-based SiNP purification procedure allowed harvesting of the membrane protein of interest even from 1000-fold dilutions.

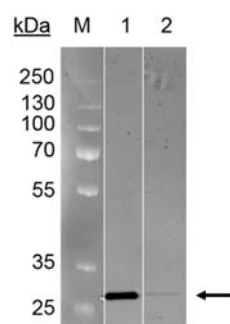


Figure 3. Western blot of SiNP-purification after sodium carbonate extraction of LHCII-PPs. Similar amounts of reaction mixture were loaded on each lane. Lane 1 shows α-PEG SiNP-purified PPs after cell-free protein synthesis. Lane 2 shows purified PPs after sodium carbonate extraction.

A suitable and well established method to confirm the orientation of LHCII integrated into polymeric membranes is the trypsin assay. Transmembrane domains and intracellular parts are protected from digestion by the membrane structure. As the VSVG-tag, which is used for antibody – based recognition, has two trypsin cleavage sites, it represents a valid target sequence for digestion. LHCII presents a total of 21 trypsin cleavage sites.

We analyzed the resulting fragment pattern in a western blot experiment with the software PeptideCutter by ExPASy (Figure 4B). The digestion pattern in Figure 4A revealed that LHCII was unidirectionally integrated in the polymeric membrane plane with the N-terminus exposed. LHCII with a VSVG-tag either on the N or C-terminus was used. Within a correctly folded and integrated LHCII only one terminus was found to be exposed to the trypsin, thus resulting in distinct digestion patterns owing to protection of transmembrane and inner parts from the protease. Western blotting experiments of trypsin treated samples revealed a protected C-terminus with a digestion pattern corresponding to correctly inserted LHCII proteins. These findings suggest directed LHCII insertion during cell-free protein synthesis. The addition of full pigment extract from pea leaves to the PPs resulted in no change in digestion protection although chlorophylls and carotenoids are essential for complete folding of LHCII *in vivo* and *in vitro*.^[22]

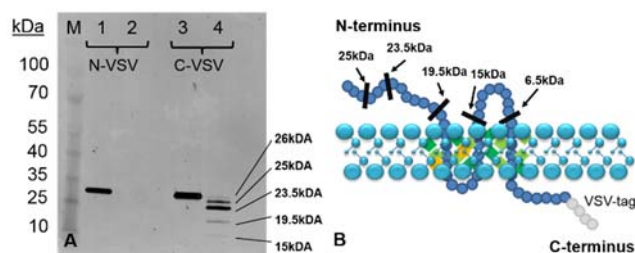


Figure 4. A) Prolonged digestion for 30 min of purified samples. Lanes 1 and 4 show untreated PPs while lanes 2 and 5 show samples digested with trypsin. Prolonged treatment with trypsin resulted in a distinct digestion pattern for C-VSVG LHCII. B) An overview of the LHCII orientation of C-VSVG labeled LHCII and relevant cleavage sites.

Although the data suggest that LHCII was successfully inserted into the polymersome membrane, the question arose as to whether the protein is able to successfully bind chlorophylls and carotenoids as it does in the native settings of the thylakoid membrane. Owing to the intrinsic hydrophobic character of chlorophylls, a detectable amount is integrated into the polymersomal membrane even in the absence of LHCII. However the presence of LHCII increases the local accumulation of chlorophylls, with the LHCII moieties gathering the chlorophylls from the hydrophobic core of the polymeric membrane. Chlorophylls as well as carotenoids were extracted from pea leaves and were subsequently added to the iMAPS of LHCII. The samples were probed for fluorescence emission specific for *Chl a*. Comparative measurements showed increased characteristic chlorophyll fluorescence emission, thus suggesting LHCII-mediated orientation of pigments that matches the physiological status in the thylakoid.

In view of the successful assembly of LHCII light harvesting complexes in the polymersomes, we transformed the spherical architectures of PPs to planar polymeric membranes, organized on solid-supported surfaces. For an efficient and strong polymer binding to the gold-coated SPR surface, the polymer material was modified with thiolated lipoic acid^[23] enabling layer formation through binding of the sulfur groups to the gold surface. Protein synthesis and pigment incubation were separated in two steps. Protein synthesis was performed for 4 hours at room temperature *in situ*. As a negative control, iMAPS was performed in the absence of any cDNA. Layer formation and subsequent modification was recorded as a function of optical thickness by using a self-made SPR setup (data not shown). Notably, a smaller increase in optical thickness was recorded in the case of LHCII expression, thus suggesting that LHCII integration reduces the surface area available for nonspecific adsorption.

The surface plasmons generated by the HeNe Laser (632.8 nm) are able to excite the *Chl b*. Since chlorophylls *a* and *b* are oriented by LHCII, the energy from *Chl b* should be transferred to a neighboring *Chl a*, from which it is emitted in the native thylakoid context as a photon with a wavelength of 670 nm. This specific excitation transfer phenomenon was observed in our experimental setting based on iMAPS – functionalized polymeric membranes (Figure 5).

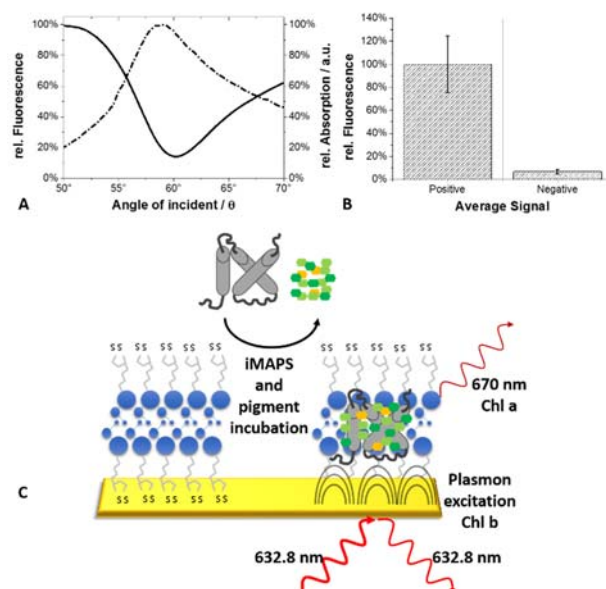


Figure 5. Surface-plasmon-induced energy transfer from *Chl b* to *Chl a*. A) An example of energy transfer within the polymer bilayer in the presence of LHCII. B) A detailed comparison of the average measured *Chl a* fluorescence upon *Chl b* excitation. (n=4) C) Representative fluorescence spectra in accordance to the surface modification.

To evaluate the specific effect of LHCII presence in the membrane, we employed an alternative membrane protein claudin2 (Cldn2) as a reference protein of human origin with no known affinity for chlorophyll interaction. In the presence of LHCII, the *Chl a* fluorescence significantly increases upon *Chl b* excitation, while with Cldn2, the fluorescence emission of the membrane surfaces decreases significantly over several independent measurements (Figure 6). This finding indicates that the increase in *Chl a* fluorescence is related to the proper arrangement of the pigments in presence of LHCII. Reversibility of fluorescence emission after photobleaching was achieved through pigment exchange, thus demonstrating reusability of the polymeric membrane surface as a novel property compared with the standard lipid- or detergent-based LHC – containing arrays.

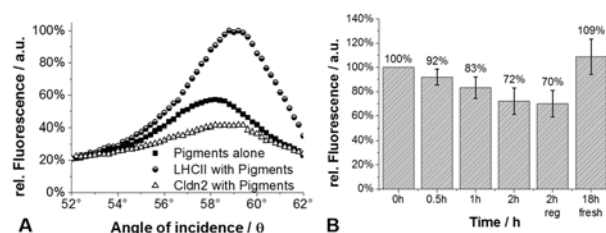


Figure 6. A) Comparative analysis of LHCII and Cldn2 shows the LHCII dependent rearrangement of chlorophylls to facilitate an energy transfer from *Chl b* to *Chl a* (n=3). B) Reversibility of fluorescence emission after photobleaching was performed through incubation with fresh pigment solution. (n=4)

In conclusion, we have demonstrated the suitability of polymersomes for the directed integration of LHCII into a robust polymeric membrane, in both spherical and planar configurations. The chlorophyll - binding capacity of LHCII was shown through fluorescence emission in an SPFS configuration. The results suggest that *in vitro* synthesized LHCII is functionally embedded in a robust and reproducible polymeric membrane with the ability to exchange chlorophylls after photobleaching. Moreover iMAPS-derived LHCII is able to bind pigments in a similar way to that found in the chloroplasts of living cells. These

findings represent a further step towards the aim of utilizing solar energy by using bioinspired recyclable materials from sustainable sources.

Experimental Section

Polybutadiene₁₂₀₀-polyethylene oxide₆₀₀ (PolymerSource) was dissolved alone or together with pigment extract in chloroform (≥99%, Roth) and prepared by film rehydration^[24] and subsequent extrusion. Pigments were extracted as described by Paulsen et al.^[6] Polymer modification with lipoic acid for formation of tethered bilayers was done as described by Belegriinou et al.^[23].

Proteins and PPs were prepared using the TNT-coupled transcription-translation wheat germ extract system (Promega, L4140). Protein was expressed in the presence or absence of pigment extract. For digestion assays, trypsin (0.5% Trypsin-EDTA, Gibco) was used. Monoclonal mouse anti-VSVG antibody (Sigma-Aldrich, VSVG = Vesicular Stomatitis Virus Glycoprotein) was used as the primary antibody and goat anti-mouse IgG labelled with infrared fluorescence dye (IRDye 800CW, Licor) was used as the secondary antibody. The antibody detection was achieved by using the Odyssey infrared imaging system (Licor).

For TEM analysis, rabbit anti-LHCII primary antibody (1 µg/ml) and immunogold-labelled goat anti-rabbit antibody (5 nm colloidal gold, Sigma) secondary antibody, as well as Uranyl acetate and OsO₄ membrane staining, were used. Another approach was to simply stain purified polymersomic membrane with OsO₄, leaving proteins unstained.

PP purification was achieved by microfiltration with Amicon® filter (Ultrafree-MC-VV, Durapore® PVDF 0.1 µm)^[9] and SiNP immunoprecipitation as described elsewhere.^[20] In case of tethered polymer bilayers, gold coated (50 nm) glass surfaces were used and SPR/SPFS experiments were performed within a self-build set-up. Fluorescence measurements were made using the Luminescence Spectrometer (LS 55, PerkinElmer Instr.).

Acknowledgements

We thank the Ministry of Transportation and Innovation, BMVIT, Austria, for financial support of the International Graduate School (IGS). We thank Prof. Walter Hunziker, ASTAR Singapore, for the Cldn2 cDNA for use as a reference protein and Christoph Zaba, University of Natural Resources and Life Science Vienna for synthesis of lipoic acid modified block copolymer.

Keywords: Light Harvesting Complex • Synthetic polymer membranes • Membrane protein expression

- [1] Z. Liu, H. Yan, K. Wang, T. Kuang, J. Zhang, L. Gui, X. An, W. Chang, *Nature* **2004**, 428, 287–292.
- [2] D. Reinsberg, P. J. Booth, C. Jegerschöld, B. J. Khoo, H. Paulsen, *Biochemistry (Mosc.)* **2000**, 39, 14305–14313.
- [3] C. Yang, R. Horn, H. Paulsen, *Biochemistry (Mosc.)* **2003**, 42, 4527–4533.
- [4] C. Yang, S. Boggasch, W. Haase, H. Paulsen, *Biochim. Biophys. Acta BBA - Bioenerg.* **2006**, 1757, 1642–1648.
- [5] N. S. Lewis, D. G. Nocera, *Proc. Natl. Acad. Sci. U. S. A.* **2006**, 103, 15729–15735.
- [6] H. Paulsen, U. Rümmler, W. Rüdiger, *Planta* **1990**, 181, 204–211.
- [7] A. Mershin, K. Matsumoto, L. Kaiser, D. Yu, M. Vaughn, M. K. Nazeeruddin, B. D. Bruce, M. Graetzel, S. Zhang, *Sci. Rep.* **2012**, 2, 234.
- [8] S. May, M. Andreasson-Ochsner, Z. Fu, Y. X. Low, D. Tan, H.-P. M. de Hoog, S. Ritz, M. Nallani, E.-K. Sinner, *Angew. Chem. Int. Ed.* **2013**, 52, 749–753.
- [9] M. Nallani, M. Andreasson-Ochsner, C.-W. D. Tan, E.-K. Sinner, Y. Wisantoso, S. Geifman-Shochat, W. Hunziker, *Biointerphases* **2011**, 6, 153–157.
- [10] R. Sachse, S. K. Dondapati, S. F. Fenz, T. Schmidt, S. Kubick, *FEBS Lett.* **2014**, 588, 2774–2781.
- [11] A. Nozawa, T. Ogasawara, S. Matsunaga, T. Iwasaki, T. Sawasaki, Y. Endo, *BMC Biotechnol.* **2011**, 11, 35.
- [12] B. M. Discher, Y. Y. Won, D. S. Ege, J. C. Lee, F. S. Bates, D. E. Discher, D. A. Hammer, *Science* **1999**, 284, 1143–1146.
- [13] M. Antonietti, S. Förster, *Adv. Mater.* **2003**, 15, 1323–1333.
- [14] R. Rodríguez-García, M. Mell, I. López-Montero, J. Netzel, T. Hellweg, F. Monroy, *Soft Matter* **2011**, 7, 1532–1542.
- [15] G. Ishihara, M. Goto, M. Saeki, K. Ito, T. Hori, T. Kigawa, M. Shirouzu, S. Yokoyama, *Protein Expr. Purif.* **2005**, 41, 27–37.
- [16] M. A. Goren, B. G. Fox, *Protein Expr. Purif.* **2008**, 62, 171–178.
- [17] C. Tan, S. Saurabh, M. P. Bruchez, R. Schwartz, P. Leduc, *Nat. Nanotechnol.* **2013**, 8, 602–608.
- [18] K. S. Drese, D. Latta, A. Murr, M. Ritz-Lehnert, E. K. Sinner, *US 20130203110 A1*, Google Patents, **2013**.
- [19] D. Christensen, C. Foged, I. Rosenkrands, H. M. Nielsen, P. Andersen, E. M. Agger, *Biochim. Biophys. Acta* **2007**, 1768, 2120–2129.
- [20] T. Zapf, C. Zafiu, C. Zaba, C.-W. D. Tan, W. Hunziker, E.-K. Sinner, *Biomater. Sci.* **2015**, DOI 10.1039/C5BM00133A.
- [21] Y. Fujiki, A. L. Hubbard, S. Fowler, P. B. Lazarow, *J. Cell Biol.* **1982**, 93, 97–102.
- [22] H. Paulsen, B. Finkenzeller, N. Kühlein, *Eur. J. Biochem. FEBS* **1993**, 215, 809–816.
- [23] S. Belegriinou, J. Dorn, M. Kreiter, K. Kita-Tokarczyk, E.-K. Sinner, W. Meier, *Soft Matter* **2010**, 6, 179–186.
- [24] M. Traikia, D. E. Warschawski, M. Recouvreur, J. Cartaud, P. F. Devaux, *Eur. Biophys. J. EBJ* **2000**, 29, 184–195.

Supporting Information

Polymer (PBD-1200-PEO-600, PolymerSource) was dissolved in chloroform ($\geq 99\%$, Roth) either alone or together with pigment extract (molecular ratio 200:1). Polymersomes were prepared by film rehydration in ultrapure water, followed by five freeze-thaw cycles in liquid nitrogen and heated in a sonicator bath at 37°C to form unilaminar polymersomes.^[1] Either ultrapure water or 0.4 M trehalose in water was used as the rehydration solution. For a uniform size distribution polymersomes were extruded through a 200 nm or 400 nm pore-sized membrane (AVESTIN, Polycarbonate membrane, 0.75 μm). Dynamic light scattering data obtained with the Zetasizer Nano ZS, show polydispersity of 0.26 ± 0.02 indicating a narrow size distribution and unilaminarity of the polymersomes.

Polymer modification, for formation of tethered bilayers, with lipoic acid was done as described by Belegriou et al.^[2] Shorty lipoic acid, N-(3-dimethylaminopropyl)-N'-ethylcarbodiimide hydrochloride (EDC) and 4-(dimethylamino) pyridine were mixed and vacuum dried for 2 h and then dissolved in dichloromethane (DCM). Parallel PBD1200-PEO600 (PolymerSource) was also vacuum dried, subsequently dissolved in DCM, mixed with triethylamine and the injected into the first flask containing the lipoic acid. The reaction mixture was stirred at room temperature for 76 h. The solution was then washed three times with saturated NaHCO_3aq , 10 % HClaq and distilled water. MgSO_4 was used to dry the organic phase, followed by filtering and evaporation of the remaining solvent.

WinSpall simulation of the polymer layer assembly measured in ethanol resulted into a thickness of 9 nm indicating bilayer formation.^[3] The same parameters were used as previously described by Dorn et al.^[4]

Proteins and proteopolymersomes (PPs) were prepared using the TNT® coupled transcription-translation wheat germ extract system (Promega, L4140). Reaction mixtures of 10 – 20 μl were prepared according to the manufacturer's protocol with addition of polymersomes (0.1 – 1 μg per μl reaction mixture).

Protein was expressed in the presence or absence of pea-derived full pigment extract. Pigments were extracted as described by Paulsen et al.^[5] Due to the poor water solubility of plant pigments they were dissolved in 96% ethanol at a concentration of 2 mg/ml and then added to the reaction mixture to a final concentration of 0.5% (v/v). The time dependent interaction of pea-derived full pigment extract with polymersomic membranes in aqueous solutions was investigated. *Chl a* fluorescence was used as representative for the pigment mixture, for it makes up for 66.5% of the used pigment extract. Within ethanol chlorophyll is fluorescence while strongly diluted in water its fluorescence is lost although its solubility remains at the chosen concentration. Chlorophyll fluorescence in 0.5% ethanol is significantly regained after addition of normal polymersomes as shown in Figure 1S/A. Over time an increase in fluorescence was observed indicating interactions of pigments with the hydrophobic part of the polymers. To achieve a more detailed measurement profile the viscosity of the aqueous solution was increased through the addition of poly-ethylene-glycol (PEG) up to a concentration of 10% w/v (Figure 1S/B). A slower time dependent fluorescence increase was observed indicating that over time more and more pigments become associated with the membrane through random diffusion, and regain their fluorescence, demonstrating that time is a crucial factor for the formation of LHCII-pigment complexes within the polymeric membrane.

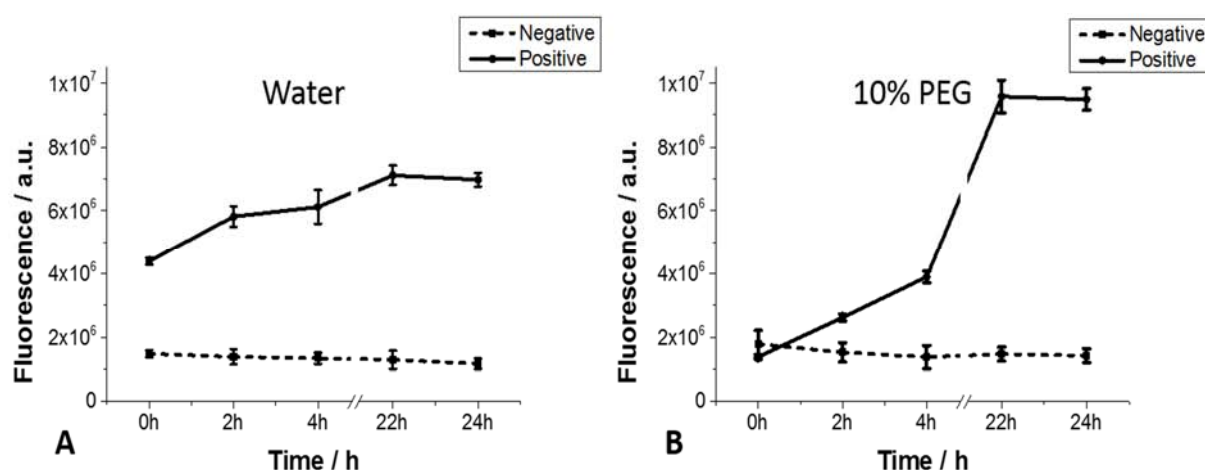


Figure 1S: Fluorescence of *Chl a* in A) water or B) 10% PEG with or without addition of 5 μ g polymer per 100 μ l mixture. Increases in fluorescence in the presence of polymersomes indicate an integration of *Chl a* over time. From the increased viscosity in the PEG solution it becomes obvious that more and more pigments are integrated over time until a certain threshold is reached. (n=4)

Based on the results obtained an overnight incubation (16-18h) of pigments was used in further surface plasmon resonance (SPR) and surface plasmon enhanced fluorescence spectroscopy (SPFS) experiments.

Successful expression of LHCII as well as products of the digestion assays were probed for using reducing SDS-PAGE and Western blotting. The amount of sample loaded onto the SDS-PAGE corresponds to 10 µl of iMAPS reaction mixture.

Transfer of protein from the electrophoretic gel to the nitrocellulose membrane was performed using the iBlot® system (Life Technologies) with subsequent blocking of the membrane for 30 minutes at room temperature with Odyssey® blocking solution (Licor). Monoclonal mouse anti-Vesicular Stomatitis Virus Glycoprotein (VSV) antibody (Sigma-Aldrich) was used as the primary antibody and goat anti-mouse IgG (IRDye 800CW, Licor) was used as the secondary antibody. The primary antibody was diluted in Odyssey® blocking solution while the secondary antibody was diluted in 50% (v/v) Odyssey® blocking solution in PBS. Incubation of the membrane with primary antibodies at 0.1 µg/ml for 1 h at room temperature was followed by five times of washing for 5 min each with 0.01% (v/v) Tween 20 (Sigma) in PBS, pH 7.4 (PBST). Incubation of the membrane with secondary antibodies at 0.1 µg/ml was performed for 1 h at room temperature. After three washing steps in PBST and two in PBS the membranes were air-dried and then analyzed using the Odyssey® infrared imaging system (Licor).

For the Amicon® centrifugal microfiltration of PPs as described by Nallani *et al.*^[6], the proteopolymersome-containing cell-free protein synthesis reaction mix was first diluted to 500 µl with PBS and then loaded onto an Amicon® filter (Ultrafree®-MC-VV, Durapore® PVDF 0.1 µm). The purification was done by centrifugation for 15 – 45 min at 600 x g until only a small retentate remained in the upper compartment. For digestion assays, 10µl of centrifugal microfiltration purified PPs sample containing 1µl trypsin (0.5% Trypsin-EDTA, Gibco) was incubated for 10 min at 37°C. In the case of extended digestion, the purified PPs were treated with 2 µl trypsin and incubated for 30 min at 37°C. Virtual digestion of the protein was done using the online program PeptideCutter by ExPASy. The fragment selection after the virtual digestion was performed under the assumption that starting from the transmembrane

sequences the luminal parts are protected while the N-terminus of the protein is exposed.

Unpurified samples without polymersomes treated with trypsin showed a signal reduction for N-VSV LHCII compared to the untreated sample while for C-VSV LHCII an additional band appeared, indicating a limited access to the tag. The same samples containing polymersomes showed a further reduced signal for N-VSV LHCII. For C-VSV appearance of two distinct additional bands was observed. Both results indicate an increased accessibility for trypsin to the protein. After trypsin treatment of centrifugal microfiltration-purified N-VSV LHCII PPs, no signal was detectable while C-VSV LHCII PPs displayed an additional band (Figure 2S). These results indicated that the N-terminus is exposed while the C-terminus remains protected within the polymersomes.

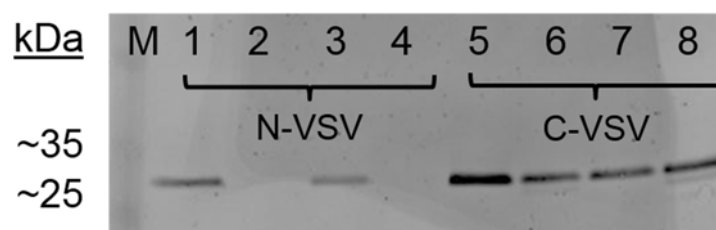


Figure 2S: Western blots of digestion assays showed a directed insertion of LHCII into polymersomes during cell free synthesis. PPs were purified using centrifugal microfiltration. Lanes 1, 3, 5 and 7 show samples not treated with trypsin. In addition, Lanes 3 and 7 show PPs incorporated with pigments. Lanes 2 and 6 as well as 4 and 8 are the respective 10 min trypsin-digested samples. The data indicate directed insertion.

For transmission electron microscopy (TEM), LHCII proteopolymersomes, synthesized with either ultrapure water or 0.4 M trehalose, were prepared as described above and immunogold-labelled using rabbit anti-LHCII antibodies (1 µg/ml in Carl Roth Roti®-Block, Mainz, Harald Paulsen) as the primary antibody and immunogold-labelled goat anti-rabbit antibody (5 nm colloidal gold, Sigma, 1:100 diluted in Roti®-Block, Carl Roth) as the secondary antibody. The incubation and blocking of the TEM grids was done in a similar manner as Western blotting described above. Antibody incubation times were reduced to 30 min each, followed by 15 min of 2.5% glutaraldehyde fixation. Proteins were stained by 10 min incubation with 1% Uranyl acetate. For the staining of the polymersome membranes 1 h incubation with 1% OsO₄ and three subsequent washing steps in ultrapure water were performed. Another approach was to simply stain the centrifugal microfiltration-

purified polymersomic membrane with 1% OsO₄ for 15 min, leaving proteins unstained.

Surface plasmon resonance was performed on dextran-coated gold surfaces (CM5, Biacore). These were used for antibody immobilization via EDC/N-hydroxysuccinimide (NHS) coupling within a Biacore 2000 setup. The channels were treated for 10 min at a flow rate of 5 µl/min with 10 µg/ml of antibody solution containing either anti-VSV antibodies (Sigma) or human IgG (negative control, Sigma). Alternatively as a second negative control one channel was deactivated immediately without treatment with antibody. Before sample measurement 5% (w/v) milk solution, (filtered through a 0.2 µm pore-sized syringe filter) was applied to the channels for 10 min at a flow rate of 2 µl/min, followed by 5 min of rinsing the channels with polymersome solution at a flow rate of 2 µl/min. Binding to the surface was indicated by a change in response unit (RU).

Orientation and insertion of LHCII moieties into polymersomes was probed using surface plasmon resonance (SPR) in combination with affinity tag – labelling as two different cDNAs coding for the LHCII were employed: one with N – terminus labelled and the alternative C – terminal labelling with the VSV – affinity peptide motif. SPR was done in the microfluidics of a BIAcore 2000 device through binding of PPs to an anti-VSV antibody-coated gold – aminodextrane functionalized SPR – chip surfaces (CM5 chip). Purified PPs resulted in binding signals 62.2 ± 3.5 RU for N-VSV and 52.1 ± 0.9 RU for C-VSV, respectively). As N- and C-VSV-labelled LHCII PPs were both able to bind to the anti-VSV antibody indicates random protein orientation. Due to the high shear force in the microfluidics of the Biacore device, the strong shear forces bursted the PPs, resulting in detection of outside – in and inside – out oriented membrane fragments, containing the LHCII.

Immunoprecipitation of protein and proteopolymersomes using antibody-functionalized silica nanoparticles (SiNPs) was performed as described in Zapf *et al.*^[7] Antibodies were immobilized through EDC/NHS coupling onto aminated SiNP surfaces as described elsewhere.^[7] Briefly, 50 µg of freshly prepared SiNPs were added to 1 ml of PBS containing 10µl of cell-free protein synthesis reaction mixture. This mixture was then incubated for 1 h at room temperature with gentle agitation. Centrifugation at 1700 x g for 5 min was used to pellet the SiNPs. These were

subsequently treated with 100 mM NaOH to achieve protein or polymersome release. Alternatively, the SiNP complexes were treated with 10% PEG (MW 8000, Sigma) for 1 h at room temperature as a competitive release method.

For sodium carbonate extraction, 10 μ l of cell-free protein synthesis reaction mix containing 10 μ g of polymersomes were added to 1 ml of 200 mM sodium carbonate, pH 11.5 and incubated on ice for 1 h. This was followed by the addition of 100 μ g of α -PEG-SiNPs and incubation for 1 h at room temperature. As a second approach to create more favorable antibody binding conditions, the 10 μ l cell-free protein synthesis reaction mixes were incubated in 1 ml of sodium carbonate buffer solution and then diluted with 9 ml of PBS prior to immunoprecipitation. The silica nanoparticles were then pelleted by centrifugation at 1700 – 2000 x g for 5 min. Further analysis was performed directly on the SiNP pellets by SDS-PAGE and Western blotting. Successful α -PEG-SiNP purification of 1 000 x times diluted samples in PBS/sodium carbonate mixture could be achieved, resulting into a similar strong band than observed for purification directly within the sodium carbonate buffer.

We performed the fluorescence measurements of immunoprecipitation-purified polymersomes using the Luminescence Spectrometer (LS 55, PerkinElmer Instr.) within disposable microcuvettes (Carl Roth, z = 8.5 mm). Purification was done using immunoprecipitation with 50 μ g of α -PEG SiNPs for 10 μ l reaction mixtures containing 2 μ g of polymersomes and using 100 μ l of 0.1 M NaOH for protein and proteopolymersome release. The purified samples were then excited at 350 - 480 nm while fluorescence emission was measured at 660-670 nm, which correlates with the emission maxima of *Chl a* when integrated into polymersome membranes. *Chl b* fluorescence emission was measured at 650 nm with the excitation wavelength of 450 nm. For analysis of energy transfer the fluorescence at 670 nm was compared to that at 650 nm after 450 nm excitation.

Figure 3S shows increased *Chl a* fluorescence at 660 nm emission (max. emission shift of spectra from 670 nm to 660 nm in 0.1 M NaOH) in purified PPs when compared to similarly-purified polymersomes lacking LHCII. Comparative analysis of chlorophylls mixed with polymersomes in the absence of LHCII and subsequently treated with 100 mM NaOH solution show a strong shift in the spectra towards max. emission at 650 nm upon excitation at 410 nm. Although after SiNP purification of the cell-free reactions lacking LHCII, no significant fluorescence level could be measured.

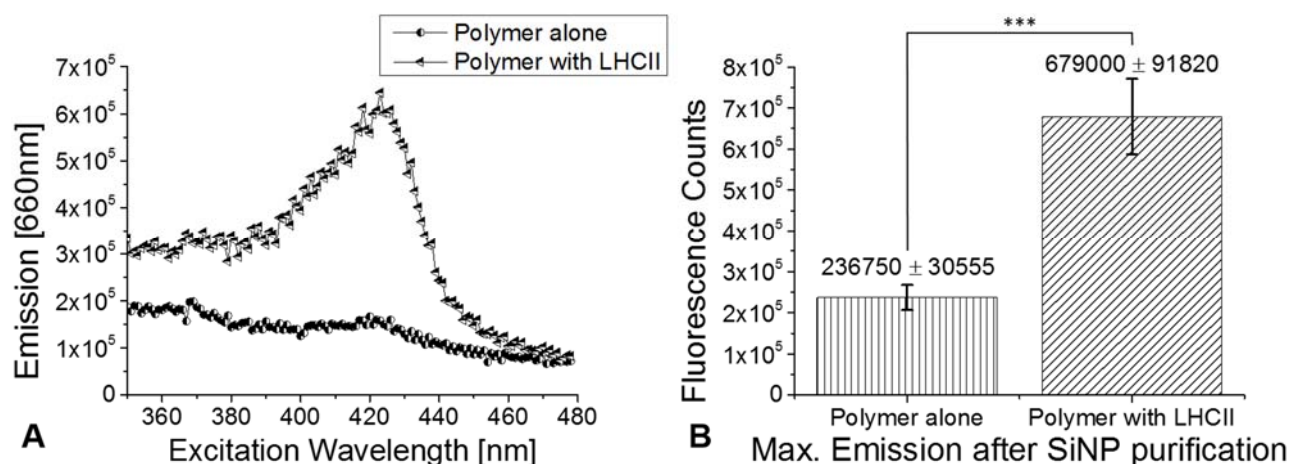


Figure 3S: Fluorescence of Chl a in the presence and absence of LHCII measured within the SiNP release solution 100 mM NaOH. A) shows an averaged fluorescence profile at the emission wavelength at 660 nm upon excitation from 350 to 480 nm. B) shows in more detail the difference in max. emission measured. (n=3, Student t-test, $p < 0.001$) The fluorescence is overall reduced and the maximum emission peak shifted the longer the exposure to NaOH.

The alternative competitive release method using a 10% PEG solution resulted in less efficient polymersome release and increased batch to batch variation. Subsequent analysis of the signals indicated possible energy transfer among the chlorophyll pigments in the presence of LHCII, introduced by iMAPS into the polymeric membrane architecture. It is notable, that sometimes, such transfer was observed even without presence of LHC protein, as the hydrophobic core of the polymersomal architecture efficiently assembled chlorophyll molecules in quite high concentration from aqueous environment.

A self-build SPR set up was used for the performed experiments, giving the advantage of direct access to the chip as well as opening the opportunity for surface plasmon enhance fluorescence spectroscopy (SPFS). As laser source a HeNe laser (JDSU HeNe Laser, Model 1125P, 5 mW Linear Polarization) with a wavelength of 632.8 nm was used. Sensor Chips were prepared by coating glass chips with 50 nm of Au. Tethered bilayer were self-assembled through ethanol dissolved incubation with 0.1 mg/ml 96% ethanol dissolved BDLA for 16 to 18 h at room temperature or 4°C in the fridge followed by intense washing with 96% ethanol and subsequent water. Sensor chip modification was done inside the SPR chamber for a precise investigation of the changes due to the modifications as well as outside the device to achieve a higher throughput. In both cases drying out of the chip had to be avoided

otherwise a thick unstructured layer of BD-LA was formed, making the chip unusable. In case of outside modification, small PDMS chambers were formed within which the bilayer formation was done. To prevent the samples from drying out, gold chips were placed into a Petri dish filled with a few ml of pure ethanol, to create a saturated atmosphere, and tightly sealed with Parafilm and stored at 4°C in the fridge for 18 hours. To ensure proper coating of the surface further incubation with 1 mg/ml 200 nm sized polymersomes was performed, followed by intense washing with water. Before wheat germ based cell free protein synthesis (L4140, Promega) was performed directly on the bilayered surface, the channel was cleared from water by blow-drying to prevent dilution of the reaction mixture. The synthesis was performed at room temperature for 4 h either without plasmid DNA or plasmids encoding for LHCII. After subsequent washing in water, incubation of with pea derived whole pigment extract 20µg/ml in water-ethanol solution (pre dissolved in 96% ethanol and subsequent dilution with water to 0.5% ethanol) was performed for 16 to 18 h, followed by intensive rinsing with water.

The surface plasmons created through laser excitation were used to excite *Chl b* at its second absorption peak. The detection of fluorescence emission was done by a photomultiplier with two emission filters upstream. Either one long pass filter with a cut-off of 650nm (Thorlabs) preventing excitation light from altering the results and a second a bandpass filter allowing only light with a wavelength of 670 ±10nm (Thorlabs) to pass through or alternatively only one bandpass filters was used resulting into a comparable measurement quality. Therefore only light emitted by *Chl a* is detected.

For the comparative analysis of pigment interaction with LHCII and Cldn2. The membrane incubation with dissolved pigments was done prior cell-free synthesis. The bleaching for the regeneration experiments was achieved through plasmon excitement at angle of maximum light adsorption on the gold surface. The regeneration step was done by incubating the chip in the dark. For a regeneration and exchange of pigments in the membrane the prepared samples were incubated again with freshly prepared pea derived whole pigment extract as described before.

For any technological application the stability of the LHCII-pigment complex within the membrane is crucial therefor its resistance and fluorescence recoverability was probed for using SPFS and surface plasmon induced bleaching at the angle of maximum laser light absorption. Due to the small chamber size used, most of the

modified surface area was exposed to bleaching process of up to 2 hours, resulting in no recovery of fluorescence after incubation in the dark. This indicates partial destruction of the chlorophylls within the membrane. Incubation with fresh pigment solution (same concentration as used before) was successfully used to recovery of the initial fluorescence levels.

[1] M. Traïkia, D. E. Warschawski, M. Recouvreur, J. Cartaud, P. F. Devaux, *Eur. Biophys. J. EBJ* 2000, 29, 184–195.

[2] S. Belegriou, J. Dorn, M. Kreiter, K. Kita-Tokarczyk, E.-K. Sinner, W. Meier, *Soft Matter* 2010, 6, 179–186.

[3] P. J. Photos, L. Bacakova, B. Discher, F. S. Bates, D. E. Discher, J. Control. Release Off. J. Control. Release Soc. 2003, 90, 323–334.

[4] J. Dorn, S. Belegriou, M. Kreiter, E.-K. Sinner, W. Meier, *Macromol. Biosci.* 2011, 11, 514–525.

[5] H. Paulsen, U. Rümmler, W. Rüdiger, *Planta* 1990, 181, 204–211.

[6] M. Nallani, M. Andreasson-Ochsner, C.-W. D. Tan, E.-K. Sinner, Y. Wisantoso, S. Geifman-Shochat, W. Hunziker, *Biointerphases* 2011, 6, 153–157.

[7] T. Zapf, C. Zafiu, C. Zaba, C.-W. D. Tan, W. Hunziker, E.-K. Sinner, *Biomater. Sci.* 2015, 3, 1279–1283.

4. Conclusion

In this work, the insertion of LHCII-pigment complexes into polymeric membranes as means of stabilization was investigated. The protein expression was performed using *in vitro* membrane-assisted protein synthesis (iMAPS) employing a commercially available wheat germ based cell-free synthesis reaction mixture. The insertion into polymeric membranes was achieved through iMAPS meaning that the cell-free synthesis was performed in the presence of polymeric membranes. In the first step, protein expression in the presence of different concentration of polymersomes was investigated with an upper limit of 5 µg polymer per 10 µl reaction mixtures. Further increase in concentration reduced the expression efficiency of the system while lower concentrations showed slightly elevated levels demonstrating the usability of iMAPS.

First attempts to purify the resulting proteopolymersomes were done using a centrifugal microfiltration system which was already shown to successfully enable purification of iMAPS generated proteopolymersomes³¹. Employing this technique, samples were purified enough to enable SPR measurements and digestion assays. First Biacore – SPR measurements demonstrated LHCII association with the polymersomes, but interestingly they also indicated a stochastic insertion, contradictory to our expectations. This can be explained through non-specific polymer-surface interactions and possible rupturing of polymersomes due to the high shear forces within the microfluidic system of the device. More conclusive digestion assays of centrifugal microfiltration purified samples using trypsin revealed an orientated insertion into the polymeric membrane.

The expression of LHCII within the plant based cell-free system was so effective that even 5 µl of reaction mixtures resulted in observable western blot bands. Working with relative small reaction amounts of 10-20 µl resulted in difficulties of further analysis due to a loss of proteopolymersome during centrifugal microfiltration as well as the presence of remaining impurities. Therefore a new strategy of polymersome purification had to be developed based on antibody modified SiNPs.

Formation and modification of SiNPs were done with minimal costs and standard laboratory equipment, making it a promising purification method, not only for polymersomes and proteopolymersome but for any proteins with respective antibodies available. Monitoring of SiNP modification was successfully done using

DLS, Zeta potential and TEM. Functionality was tested for different polymersomes, proteopolymersomes containing LHCII and Cln2 as well as for non-integrated LHCII and Cln2.

The usage of SiNP purification system made new analysis methods possible for LHCII proteopolymersomes. Sodium carbonate extraction assay as an alternative method of integration testing confirmed the full incorporation of the membrane protein. Further SiNPs purification was compared to the previously used method of centrifugal microfiltration, demonstrating that both methods can be used in every standard molecular biology lab. However higher purification and yield was observed for SiNP usage. Nevertheless, the usage of centrifugal microfiltration should not be dismissed as it has the advantage of not needing antibodies against polymer or protein.

Functionality of reconstituted LHCII-pigment complexes is commonly analyzed by monitoring energy transfer from *Chl b* to *Chl a*.⁸ For our constructs we observed that chlorophylls integrated into the polymeric membrane even in the absence of LHCII, creating a fluorescence background. Without prior purification no significant difference in cell-free synthesized proteopolymersomes, with and without LHCII was observed. In the case of centrifugal microfiltration, significant amounts of polymersome and pigments remained in the filter membrane making the results unreliable. SiNPs on the other hand were able to purify satisfying amounts of fluorescent proteopolymersome showing that in the presence of LHCII the emitted fluorescence is significantly increased. But this method displayed a major drawback due to the harsh release conditions. The fluorescence spectra of the chlorophylls was altered, making the specific energy transfer from *Chl b* to *Chl a* unobservable. The usage of non-invasive release conditions using a competitive PEG release resulted into a poor release and strong batch to batch variations making a conclusive analysis impossible.

In an attempt to increase the density of LHCII within the polymer membrane and for more detailed characterization of LHCII-pigment-polymer constructs as well as to address possible technological applications of polymeric membranes, we moved to investigate the suitability of planar tethered polymer bilayers for our purpose. The formation of surface attached polymer bilayers by vesicle fusion as shown previously by Dorn *et al.*⁴² was rapidly dismissed as membrane removal was observed over

time. To assure proper binding of the membrane to the support, in our case gold due to SPR and SPFS analysis, polymers were modified with lipoic acid⁷⁸ to induce strong Au – S bonds. Formation of bilayer was successfully done through self-assembly in ethanol demonstrating the easy applicability of this method. Gold surface modification, LHCII synthesis and pigment integration were monitored using a self-build SPR setup. Fluorescence measurements showed that in the presence of LHCII the amount of polymer – integrating pigments drastically increased. In the case of the pigmented polymer bilayer, with and without LHCII, energy transfer was observed. Energy transfer, though, was significantly increased upon LHCII integration. The integration of Cldn2 as a control membrane protein resulted in a decrease in fluorescence, emphasizing that LHCII protein is indeed responsible for the rearrangement of pigment molecules.

Surface plasmon induced bleaching and regeneration experiments showed that polymer integrated pigments, harmed in their function, can be exchanged through incubation with a fresh pigments solution. All these findings make our construct interesting for photovoltaic and light sensor applications. Furthermore the combination of cell-free synthesis and polymeric membranes, both vesicular and planar, has a promising outlook in many areas of membrane protein research and application.

5. Abbreviations

Å	Angstrom
APTES	(3-aminopropyl) triethoxysilane
BD-LA	polybutadiene-polyethylene oxide polymer modified with lipoic acid
Chl	Chlorophyll
Chl a	chlorophyll a
Chl b	chlorophyll b
Cldn2	human claudin 2
C-VSV	VSV linked to the C-terminus
Da	Dalton
DCM	dichloromethane
DLS	dynamic light scattering
DNA	Deoxyribonucleic acid
<i>E.coli</i>	Escherichia coli
EDC	N-(3-dimethylaminopropyl)-N'-ethylcarbodiimide
GPCR	G protein–coupled receptor
GUV	giant unilaminar vesicles
HeNe	Helium-Neon (laser)
iMAPS	in vitro membrane-assisted protein synthesis
LHCII	major light-harvesting chlorophyll a/b complex II
mRNA	messengerRNA
NHS	N-hydroxysuccinimide
N-VSV	VSV linked to the N-terminus
PBD	polybutadiene
PBS	Phosphate-buffered saline

PBST	Phosphate-buffered saline with 0.1% Tween 20
PDMS	Polydimethylsiloxane
PEG or PEO	polyethylene glycol or polyethylene oxide
RU	resonance units
SDS-PAGE	sodium dodecyl sulfate polyacrylamide gel electrophoresis
SiNP	silica nanoparticle
SPFS	surface plasmon enhanced fluorescence spectroscopy
SPR	surface plasmon resonance
TEM	transmission electron microscopy
TEOS	tetraethoxysilane
VSV	vesicular stomatitis virus glycoprotein also called VSV-G
α -PEG	anti-polyethylene glycol antibody
α -VSV	anti-vesicular stomatitis virus antibody

6. List of Figures

Figure 1: Model of the quaternary structure of LHCII trimers. A) View from stromal side on a LHCII trimer with all the chlorophylls and carotenoids tightly packed. In B) the integration into the thylakoid membrane is shown.¹² (adapted from “Crystallisation, structure and function of plant light-harvesting Complex II.”, by Barros, T. & Kühlbrandt, W., 2009, *Biochim. Biophys. Acta BBA - Bioenerg.* 1787, 753–772) 9

Figure 2: Core structure of chlorophyll *a* and *b*. Only one side chain is different between *Chl a* and *Chl b* which results into altered binding properties as well as a shift in the adsorption and emission spectra.²¹ (adapted from “Chlorophyll a, b and d.” by Yikrazuul, 2009, http://commons.wikimedia.org/wiki/File:Chlorophyll_a_b_d.svg)10

Figure 3: LHCII-pigment absorbance spectra within an aqueous solution as well as in diethyl ether. The main absorbance occurs within the blue and red light range.²⁴ (adapted from “Photocurrent activity of light-harvesting complex II isolated from spinach and its pigments in dye-sensitized TiO₂ solar cell”, by Yu, D., Zhu, G., Liu, S., Ge, B. & Huang, F., 2013, *Int. J. Hydrog. Energy* 38, 16740–16748) 11

Figure 4: Energy transfer from carotenoids to chlorophylls and their different excitation levels and transfer times.²⁶ (adapted from “Carotenoid-to-chlorophyll energy transfer in recombinant major light-harvesting complex (LHCII) of higher plants. I. Femtosecond transient absorption measurements”, by Croce, R., Muller, M. G., Bassi, R. & Holzwarth, A. R., 2001, *Biophys. J.* 80, 901–915)..... 12

Figure 5: Main self-assembled structures formed by AB diblock copolymer. Depending on the dimensionless ‘packing parameter’ *p* either spherical micelles, cylindrical micelles or polymersomes form in the appropriate concentration and solution.³⁵ (adapted from „Self-Assembled Block Copolymer Aggregates: From Micelles to Vesicles and their Biological Applications”, by Blanazs, A., Armes, S. P. & Ryan, A. J., 2009, *Macromol. Rapid Commun.* 30, 267–277)..... 15

Figure 6: Schematic illustration of a Kretschmann configuration showing the propagation of surface plasmons and the resulting evanescence field on the outer side of the gold layer. The incident angle θ has to be chosen so that there is a phase match of the momentum of the light and the surface plasmons.⁶⁹ (adapted from

“Localized surface plasmon resonances in nanostructures to enhance nonlinear vibrational spectroscopies: towards an astonishing molecular sensitivity”, by Lis, D. & Cecchet, F. , 2014, *Beilstein J. Nanotechnol.* 5, 2275–2292) 18

Figure 7: Representative SPR curve. The total internal reflection resembles the point at which 100% of the light is reflected. The black line crossing the curve in the point of the black circle demonstrated a suitable angle for real time measurements due to strong changes in signal intensity upon surface changes. At the point of the lowest reflective intensity the surface plasmon resonance is the strongest. 19

7. References

1. Cashmore, A. R. Structure and expression of a pea nuclear gene encoding a chlorophyll a/b-binding polypeptide. *Proc. Natl. Acad. Sci.* 81, 2960–2964 (1984).
2. Camm, E. L. & Green, B. R. How the Chlorophyll-Proteins got their Names. *Photosynth. Res.* 80, 189–196 (2004).
3. Nussberger, S. et al. Spectroscopic characterization of three different monomeric forms of the main chlorophyll a/b binding protein from chloroplast membranes. *Biochemistry (Mosc.)* 33, 14775–14783 (1994).
4. Peter, G. F. & Thornber, J. P. Biochemical composition and organization of higher plant photosystem II light-harvesting pigment-proteins. *J. Biol. Chem.* 266, 16745–16754 (1991).
5. Ruban, A. V., Lee, P. J., Wentworth, M., Young, A. J. & Horton, P. Determination of the stoichiometry and strength of binding of xanthophylls to the photosystem II light harvesting complexes. *J. Biol. Chem.* 274, 10458–10465 (1999).
6. Dreyfuss, B. W. & Thornber, J. P. Assembly of the Light-Harvesting Complexes (LHCs) of Photosystem II (Monomeric LHC IIb Complexes Are Intermediates in the Formation of Oligomeric LHC IIb Complexes). *Plant Physiol.* 106, 829–839 (1994).
7. Sprague, S. G., Camm, E. L., Green, B. R. & Staehelin, L. A. Reconstitution of light-harvesting complexes and photosystem II cores into galactolipid and phospholipid liposomes. *J. Cell Biol.* 100, 552–557 (1985).
8. Paulsen, H., Rümmler, U. & Rüdiger, W. Reconstitution of pigment-containing complexes from light-harvesting chlorophyll a/b-binding protein overexpressed in *Escherichia coli*. *Planta* 181, 204–211 (1990).
9. Paulsen, H., Finkenzeller, B. & Kühlein, N. Pigments induce folding of light-harvesting chlorophyll a/b-binding protein. *Eur. J. Biochem. FEBS* 215, 809–816 (1993).
10. Booth, P. J. & Paulsen, H. Assembly of light-harvesting chlorophyll a/b complex in vitro. Time-resolved fluorescence measurements. *Biochemistry (Mosc.)* 35, 5103–5108 (1996).
11. Reinsberg, D., Ottmann, K., Booth, P. J. & Paulsen, H. Effects of chlorophyll a, chlorophyll b, and xanthophylls on the in vitro assembly kinetics of the major light-harvesting chlorophyll a/b complex, LHCIIb. *J. Mol. Biol.* 308, 59–67 (2001).

12. Barros, T. & Kühlbrandt, W. Crystallisation, structure and function of plant light-harvesting Complex II. *Biochim. Biophys. Acta BBA - Bioenerg.* 1787, 753–772 (2009).
13. Liu, Z. et al. Crystal structure of spinach major light-harvesting complex at 2.72 Å resolution. *Nature* 428, 287–292 (2004).
14. Yang, C., Kosemund, K., Cornet, C. & Paulsen, H. Exchange of pigment-binding amino acids in light-harvesting chlorophyll a/b protein. *Biochemistry (Mosc.)* 38, 16205–16213 (1999).
15. P07371 (CB22_PEA). Uniprot, Protein Knowledgebase (2013). at <http://www.uniprot.org/uniprot/P07371>
16. Kühlbrandt, W., Wang, D. N. & Fujiyoshi, Y. Atomic model of plant light-harvesting complex by electron crystallography. *Nature* 367, 614–621 (1994).
17. Horn, R. & Paulsen, H. Folding in vitro of light-harvesting chlorophyll a/b protein is coupled with pigment binding. *J. Mol. Biol.* 318, 547–556 (2002).
18. Yang, C., Horn, R. & Paulsen, H. The light-harvesting chlorophyll a/b complex can be reconstituted in vitro from its completely unfolded apoprotein. *Biochemistry (Mosc.)* 42, 4527–4533 (2003).
19. Hobe, S., Niemeier, H., Bender, A. & Paulsen, H. Carotenoid binding sites in LHCIIb. Relative affinities towards major xanthophylls of higher plants. *Eur. J. Biochem. FEBS* 267, 616–624 (2000).
20. Kühlbrandt, W. & Wang, D. N. Three-dimensional structure of plant light-harvesting complex determined by electron crystallography. *Nature* 350, 130–134 (1991).
21. Yikrazuul. English: chlorophyll a, b and d. (2009). at http://commons.wikimedia.org/wiki/File:Chlorophyll_a_b_d.svg
22. Giuffra, E., Cugini, D., Croce, R. & Bassi, R. Reconstitution and pigment-binding properties of recombinant CP29. *Eur. J. Biochem. FEBS* 238, 112–120 (1996).
23. Tanaka, R. & Tanaka, A. Chlorophyll cycle regulates the construction and destruction of the light-harvesting complexes. *Biochim. Biophys. Acta BBA - Bioenerg.* 1807, 968–976 (2011).
24. Yu, D., Zhu, G., Liu, S., Ge, B. & Huang, F. Photocurrent activity of light-harvesting complex II isolated from spinach and its pigments in dye-sensitized TiO₂ solar cell. *Int. J. Hydrog. Energy* 38, 16740–16748 (2013).

25. Alberts, B. et al. *Molecular Biology of the Cell*. (Garland Science, 2008).
26. Croce, R., Muller, M. G., Bassi, R. & Holzwarth, A. R. Carotenoid-to-chlorophyll energy transfer in recombinant major light-harvesting complex (LHCII) of higher plants. I. Femtosecond transient absorption measurements. *Biophys. J.* 80, 901–915 (2001).
27. Cho, F. & Govindjee. Low-temperature (4–77°K) spectroscopy of chlorella; temperature dependence of energy transfer efficiency. *Biochim. Biophys. Acta BBA - Bioenerg.* 216, 139–150 (1970).
28. Discher, B. M. et al. Polymersomes: tough vesicles made from diblock copolymers. *Science* 284, 1143–1146 (1999).
29. May, S. et al. In Vitro Expressed GPCR Inserted in Polymersome Membranes for Ligand-Binding Studies. *Angew. Chem. Int. Ed.* 52, 749–753 (2013).
30. Andreasson-Ochsner, M. et al. Selective Deposition and Self-Assembly of Triblock Copolymers into Matrix Arrays for Membrane Protein Production. *Langmuir* 28, 2044–2048 (2012).
31. Nallani, M. et al. Proteopolymersomes: in vitro production of a membrane protein in polymersome membranes. *Biointerphases* 6, 153–157 (2011).
32. Antonietti, M. & Förster, S. Vesicles and Liposomes: A Self-Assembly Principle Beyond Lipids. *Adv. Mater.* 15, 1323–1333 (2003).
33. Rodríguez-García, R. et al. Polymersomes: smart vesicles of tunable rigidity and permeability. *Soft Matter* 7, 1532–1542 (2011).
34. Nardin, C., Hirt, T., Leukel, J. & Meier, W. Polymerized ABA Triblock Copolymer Vesicles. *Langmuir* 16, 1035–1041 (1999).
35. Blazs, A., Armes, S. P. & Ryan, A. J. Self-Assembled Block Copolymer Aggregates: From Micelles to Vesicles and their Biological Applications. *Macromol. Rapid Commun.* 30, 267–277 (2009).
36. Reinecke, A. A. & Döbereiner, H.-G. Slow Relaxation Dynamics of Tubular Polymersomes after Thermal Quench. *Langmuir* 19, 605–608 (2003).
37. Zhong, S., Cui, H., Chen, Z., Wooley, K. L. & Pochan, D. J. Helix self-assembly through the coiling of cylindrical micelles. *Soft Matter* 4, 90–93 (2007).

38. Photos, P. J., Bacakova, L., Discher, B., Bates, F. S. & Discher, D. E. Polymer vesicles in vivo: correlations with PEG molecular weight. *J. Control. Release Off. J. Control. Release Soc.* 90, 323–334 (2003).
39. Bermudez, H., Brannan, A. K., Hammer, D. A., Bates, F. S. & Discher, D. E. Molecular Weight Dependence of Polymersome Membrane Structure, Elasticity, and Stability. *Macromolecules* 35, 8203–8208 (2002).
40. Battaglia, G., Ryan, A. J. & Tomas, S. Polymeric vesicle permeability: a facile chemical assay. *Langmuir ACS J. Surf. Colloids* 22, 4910–4913 (2006).
41. Pawar, P. V., Gohil, S. V., Jain, J. P. & Kumar, N. Functionalized polymersomes for biomedical applications. *Polym. Chem.* 4, 3160–3176 (2013).
42. Dorn, J., Belegriou, S., Kreiter, M., Sinner, E.-K. & Meier, W. Planar block copolymer membranes by vesicle spreading. *Macromol. Biosci.* 11, 514–525 (2011).
43. Discher, B. M. et al. Cross-linked Polymersome Membranes: Vesicles with Broadly Adjustable Properties. *J. Phys. Chem. B* 106, 2848–2854 (2002).
44. Meng, F., Engbers, G. H. M., Gessner, A., Müller, R. H. & Feijen, J. Pegylated polystyrene particles as a model system for artificial cells. *J. Biomed. Mater. Res. A* 70, 97–106 (2004).
45. Traïkia, M., Warschawski, D. E., Recouvreur, M., Cartaud, J. & Devaux, P. F. Formation of unilamellar vesicles by repetitive freeze-thaw cycles: characterization by electron microscopy and ³¹P-nuclear magnetic resonance. *Eur. Biophys. J. EBJ* 29, 184–195 (2000).
46. Lee, J. C. et al. Preparation, stability, and in vitro performance of vesicles made with diblock copolymers. *Biotechnol. Bioeng.* 73, 135–145 (2001).
47. Marsden, H. R., Gabrielli, L. & Kros, A. Rapid preparation of polymersomes by a water addition/solvent evaporation method. *Polym. Chem.* 1, 1512–1518 (2010).
48. Belegriou, S. et al. Biomimetic supported membranes from amphiphilic block copolymers. *Soft Matter* 6, 179–186 (2009).
49. Nirenberg, M. W. & Matthaei, J. H. The dependence of cell-free protein synthesis in *E. coli* upon naturally occurring or synthetic polyribonucleotides. *Proc. Natl. Acad. Sci. U. S. A.* 47, 1588–1602 (1961).
50. Carlson, E. D., Gan, R., Hodgman, C. E. & Jewett, M. C. Cell-free protein synthesis: applications come of age. *Biotechnol. Adv.* 30, 1185–1194 (2012).

51. Nozawa, A. et al. Production and partial purification of membrane proteins using a liposome-supplemented wheat cell-free translation system. *BMC Biotechnol.* 11, 35 (2011).
52. Goren, M. A. & Fox, B. G. Wheat germ cell-free translation, purification, and assembly of a functional human stearyl-CoA desaturase complex. *Protein Expr. Purif.* 62, 171–178 (2008).
53. Ishihara, G. et al. Expression of G protein coupled receptors in a cell-free translational system using detergents and thioredoxin-fusion vectors. *Protein Expr. Purif.* 41, 27–37 (2005).
54. Shadiac, N., Nagarajan, Y., Waters, S. & Hrmova, M. Close allies in membrane protein research: cell-free synthesis and nanotechnology. *Mol. Membr. Biol.* 30, 229–245 (2013).
55. Chen, H. Z. & Zubay, G. Prokaryotic coupled transcription-translation. *Methods Enzymol.* 101, 674–690 (1983).
56. Gasior, E., Herrera, F., Sadnik, I., McLaughlin, C. S. & Moldave, K. The preparation and characterization of a cell-free system from *Saccharomyces cerevisiae* that translates natural messenger ribonucleic acid. *J. Biol. Chem.* 254, 3965–3969 (1979).
57. Erickson, A. H. & Blobel, G. Cell-free translation of messenger RNA in a wheat germ system. *Methods Enzymol.* 96, 38–50 (1983).
58. Swerdel, M. R. & Fallon, A. M. Cell-free translation in lysates from *Spodoptera frugiperda* (Lepidoptera: Noctuidae) cells. *Comp. Biochem. Physiol. B* 93, 803–806 (1989).
59. Ezure, T. et al. Cell-free protein synthesis system prepared from insect cells by freeze-thawing. *Biotechnol. Prog.* 22, 1570–1577 (2006).
60. Jackson, R. J. & Hunt, T. Preparation and use of nuclease-treated rabbit reticulocyte lysates for the translation of eukaryotic messenger RNA. *Methods Enzymol.* 96, 50–74 (1983).
61. Kobayashi, T., Mikami, S., Yokoyama, S. & Imataka, H. An improved cell-free system for picornavirus synthesis. *J. Virol. Methods* 142, 182–188 (2007).
62. Shimizu, Y., Kanamori, T. & Ueda, T. Protein synthesis by pure translation systems. *Methods* 36, 299–304 (2005).
63. Basu, D., Castellano, J. M., Thomas, N. & Mishra, R. K. Cell-free protein synthesis and purification of human dopamine D2 receptor long isoform. *Biotechnol. Prog.* 29, 601–608 (2013).

64. Sachse, R., Dondapati, S. K., Fenz, S. F., Schmidt, T. & Kubick, S. Membrane protein synthesis in cell-free systems: from bio-mimetic systems to bio-membranes. *FEBS Lett.* 588, 2774–2781 (2014).
65. Schwarz, D., Dötsch, V. & Bernhard, F. Production of membrane proteins using cell-free expression systems. *Proteomics* 8, 3933–3946 (2008).
66. Spirin, A. S., Baranov, V. I., Ryabova, L. A., Ovodov, S. Y. & Alakhov, Y. B. A continuous cell-free translation system capable of producing polypeptides in high yield. *Science* 242, 1162–1164 (1988).
67. Kim, D. M. & Choi, C. Y. A semicontinuous prokaryotic coupled transcription/translation system using a dialysis membrane. *Biotechnol. Prog.* 12, 645–649 (1996).
68. Surface plasmon resonance. Wikipedia, the free encyclopedia (2015). at <http://en.wikipedia.org/w/index.php?title=Surface_plasmon_resonance&oldid=656769203>
69. Lis, D. & Cecchet, F. Localized surface plasmon resonances in nanostructures to enhance nonlinear vibrational spectroscopies: towards an astonishing molecular sensitivity. *Beilstein J. Nanotechnol.* 5, 2275–2292 (2014).
70. Wiley: Introduction to Biophotonics - Paras N. Prasad. at <<http://as.wiley.com/WileyCDA/WileyTitle/productCd-0471287709.html>>
71. Honari, P., Allaudin, Z. N., Lila, M. a. M. & Mustafa, N. H. B. An approach towards optimal usage of immobilized sensor chips in Surface Plasmon Resonance based biosensor. *Afr. J. Biotechnol.* 10, 15795–15800 (2013).
72. Ding, X. et al. Surface plasmon resonance biosensor for highly sensitive detection of microRNA based on DNA super-sandwich assemblies and streptavidin signal amplification. *Anal. Chim. Acta* 874, 59–65 (2015).
73. Liebermann, T. & Knoll, W. Surface-plasmon field-enhanced fluorescence spectroscopy. *Colloids Surf. Physicochem. Eng. Asp.* 171, 115–130 (2000).
74. Wiltschi, B., Knoll, W. & Sinner, E.-K. Binding assays with artificial tethered membranes using surface plasmon resonance. *Methods San Diego Calif* 39, 134–146 (2006).
75. Yu, F., Yao, D. & Knoll, W. Surface plasmon field-enhanced fluorescence spectroscopy studies of the interaction between an antibody and its surface-coupled antigen. *Anal. Chem.* 75, 2610–2617 (2003).

76. Zapf, T. et al. Nanoscopic leg irons: harvesting of polymer-stabilized membrane proteins with antibody-functionalized silica nanoparticles. *Biomater. Sci.* 3, 1279–1283 (2015).
77. Ding, Shaohua. In Vitro Synthesis of the Light-Harvesting Complex into Artificial Membrane Systems. (Johannes Gutenberg-Universität Mainz, 2010).
78. Belegriou, S. et al. Biomimetic supported membranes from amphiphilic block copolymers. *Soft Matter* 6, 179–186 (2010).

Curriculum Vitae

Personal information

Name	Zapf Thomas
<u>Date of birth</u>	21.05.1988
Place of birth	Vienna
Country	Austria
Citizenship	Austria
University	University of Natural Resources and Life Science, Vienna, Austria Nanyang Technical University, Singapore

Education

2012-2015: International Graduates School in BioNanoTechnology

University of Natural Resources and Life Science Vienna, Austria and Nanyang Technical University, Singapore

2007-2012: Bachelor and Master program in Biomedical Engineering with Specialization in Cellular and Tissue Engineering

University of Applied Sciences Technikum Wien, Vienna, Austria

Professional Background

2012-2015: PhD Student within Joint-PhD Program between Austria and Singapore

University of Natural Resources and Life Science Vienna, Austria and Nanyang Technical University, Singapore

2011-2012: Master Student

University of Natural Resources and Life Science Vienna

2011-2012: Research Fellow

University of Applied Sciences Technikum Wien, Vienna, Austria

Vienna	October 2015
--------	--------------